\$ SUPER

Contents lists available at ScienceDirect

Deep-Sea Research Part I

journal homepage: www.elsevier.com/locate/dsri





Otoliths of marine fishes record evidence of low oxygen, temperature and pH conditions of deep Oxygen Minimum Zones

Leticia Maria Cavole ^{a,b,*}, Karin E. Limburg ^c, Natalya D. Gallo ^{a,d}, Anne Gro Vea Salvanes ^d, Arturo Ramírez-Valdez ^{a,e,f}, Lisa A. Levin ^a, Octavio Aburto Oropeza ^a, Andreas Hertwig ^{g,h}, Ming-Chang Liu ^g, Kevin D. McKeegan ^g

- ^a Scripps Institution of Oceanography, University of California San Diego, 9500 Gilman Drive, La Jolla, CA, 92093, USA
- ^b Wildlife, Fish and Conservation Biology, University of California Davis, Davis, CA, USA
- c Department of Environmental Biology, State University of New York College of Environmental Science and Forestry, Syracuse, NY, 13210, USA
- d Department of Biological Sciences, University of Bergen, 5020, Bergen, Norway
- e Centro de Investigación en Alimentación y Desarrollo A.C. (CIAD) Guaymas Unit, Guaymas, 85480, Sonora, Mexico
- f Giant Sea Bass Project Proyecto Mero Gigante, Ensenada, Baja California, 22860, Mexico
- g Department of Earth, Planetary, and Space Sciences, University of California Los Angeles, Los Angeles, CA, 90095, USA
- ^h Institute of Earth Sciences, Heidelberg University, 69120, Heidelberg, Germany

ARTICLE INFO

Keywords: Oxygen minimum zones (OMZs) Otolith microchemistry Deep-sea fish Hypoxia Eastern boundary upwelling systems (EBUS)

ABSTRACT

The deep-sea is rapidly losing oxygen, with profound implications for marine organisms. Within Eastern Boundary Upwelling Systems, such as the California and the Benguela Current Ecosystems, an important question is how the ongoing expansion, intensification and shoaling of Oxygen Minimum Zones (OMZs) will affect deepsea fishes throughout their lifetimes. One of the first steps to filling this knowledge gap is through the development of tools and techniques to track fishes' exposure to hypoxic (<45 µmol kg⁻¹), low-temperature (~4–10°C) and low-pH (\sim 7.5) waters when inhabiting OMZs. Here, we examine if the otoliths of deep-sea fishes living in OMZs exhibit distinct patterns of elemental and isotopic composition, which could be used to monitor their exposure history to severely hypoxic and low-pH waters. We hypothesize that the unique biogeochemistry of OMZs (i.e., low-oxygen, low-pH, and the presence of dissolved elements) will impart unique elemental and isotopic signatures upon the otoliths of both long-lived and short-lived deep-sea fishes living within it. We analyzed the otoliths of six deep-sea fish species from three OMZ regions: the Southern California Bight and the Gulf of California in the Northeast Pacific Ocean, and the Namibian shelf in the Southeast Atlantic Ocean. Three complementary techniques were applied: laser ablation inductively coupled plasma mass spectrometry, secondary ion mass spectrometry and scanning X-ray fluorescence microscopy. We observed that deep-water OMZdwelling fishes spanning a range of life-history traits (e.g., longevity, maximum size, growth rate, parental investment and thermal history inferred by δ^{18} O) exhibited a common elemental fingerprint (with respect to Sr:Ca, Mn:Ca, Ba:Ca, Cu:Ca and Mg:Ca) when compared to a shallow-water marine fish from better-oxygenated waters. Our findings suggest that the underlying mechanism for the common elemental fingerprinting of otoliths of OMZdwelling fishes is attributed to the unique biogeochemistry found on the margins of these highly productive upwelling systems as well as the physiological constraints resident organisms are perennially exposed to, including low oxygen, pH and temperature conditions.

E-mail address: lcavole@ucsd.edu (L.M. Cavole).

^{*} Corresponding author. Otolith Geochemistry and Fish Ecology Laboratory - Department of Wildlife, Fish, and Conservation Biology, West Entry Trailer offices, 1120 Orchard Rd, Davis, CA, 95616, USA.

1. Introduction

1.1. The rapid loss of oxygen in the global oceans

Ocean deoxygenation is the loss of oxygen (O_2) in the ocean (Keeling and Garcia, 2002; Keeling et al., 2010) and is driven by global warming and excess nutrient inputs (Breitburg et al., 2018). This phenomenon has resulted in the loss of 77 billion metric tons, or approximately 2% of the O_2 content in the open ocean since the 1960s (Schmidtko et al., 2017), as well as the development of hypoxic zones in more than 500 coastal sites across the globe (Breitburg et al., 2018; Pitcher et al., 2021).

Global warming is likely the primary cause of continuing deoxygenation in the open ocean and deep-sea basins. The increase of temperature decreases seawater solubility of O_2 , and it increases stratification in the upper ocean, reducing the supply of O_2 to the ocean's interior (Sarmiento et al., 1998; Keeling and Garcia, 2002). Global warming can also increase aquatic microbial, plant and animal respiration processes, which can lead to further reductions in dissolved oxygen levels. Models forecast declines in the global ocean O_2 inventory between 1 and 7% by the end of this century, mainly due to reduced transport of O_2 into the ocean interior (Keeling et al., 2010). This is expected to alter ocean productivity, biogeochemical cycles, marine habitats, and marine biodiversity (Keeling and Garcia, 2002; Stramma et al., 2012; Breitburg et al., 2018).

These predictions are particularly concerning for regions known as Oxygen Minimum Zones (OMZs). These permanent midwater features occur at approximately 100-1500 m, mainly along the Eastern Boundary Upwelling Systems (EBUS), where there is high primary productivity in surface waters, high carbon export to the deep, and slow advection of oxygen-rich deep-currents (Wyrtki, 1962). OMZs are defined by oxygen concentrations ${<}20~\mu\text{mol}~kg^{\text{-}1}$ in the Pacific and Indian Oceans and ${<}45$ μmol kg⁻¹ in the Atlantic Ocean (Gilly et al., 2013). OMZs correspond to 8% of total oceanic area and contain the largest reservoir of hypoxic waters in the world (Helly and Levin, 2004; Paulmier and Ruiz-Pino, 2009). Immediately above or below an OMZ, there is an oxygen limited zone (OLZ) characterized by oxygen concentration $<60~\mu mol$ kg⁻¹ in the Pacific and Indian Oceans and <90 μmol kg⁻¹ in the Atlantic (Gilly et al., 2013). The oxygen concentrations commonly observed in OMZs and OLZs are physiologically challenging for many marine organisms (60–120 µmol kg⁻¹) (Vaquer-Sunyer and Duarte, 2008), placing these deep-sea ecosystems as ideal regions to study severe hypoxia. OMZs are also Carbon Maximum Zones (CMZs), due to their high concentrations of dissolved inorganic carbon (DIC) and, as such, can function as "natural laboratories" to understand the interplay between low O2, low pH and high CO2 (Paulmier et al., 2011). The rapid, ongoing, and ubiquitous deoxygenation trends in the deep sea increase the need to identify which regions and marine organisms are most vulnerable to or tolerant of low oxygen and pH conditions.

1.2. Southern California Bight, Gulf of California, and Namibian shelf OMZs: unique places to study fish exposure to severe hypoxia

OMZs are not only midwater features; they intercept the shelf and slope of continental margins to create extensive severely hypoxic seafloor habitats ($<20 \, \mu \text{mol kg}^{-1}$) – an area estimated globally of 1,148,000 km² (Helly and Levin, 2004). In the California Current Ecosystem, the Southern California Bight (SCB) OMZ occurs from about 450 to 1250 m depth and is characterized by the presence of low oxygen levels on the outer continental shelf that are adverse to some demersal and epibenthic species (Levin, 2003; McClatchie et al., 2010; Sato et al., 2018; Gallo and Levin 2016; Gallo, 2018) and compress the habitat for midwater fish (Koslow et al., 2011). Between 1984 and 2006, oxygen declines of up to $\sim 2.1 \, \mu \text{mol kg}^{-1} \, \text{y}^{-1}$ (up to 21%) were observed at several stations off the coast of Southern California and were associated with a shoaling of the hypoxia boundary ($O_2 \sim 60 \, \mu \text{mol kg}^{-1}$) by up to 100 m, particularly in the nearshore regions (Bograd et al., 2008). These declines were likely

driven by the advection of modified source water, such as the California Undercurrent (Bograd et al., 2015). In the SCB OMZ, we selected species in which the adult stages are permanently or semi-permanently exposed to severe hypoxia. Shortspine thornyhead *Sebastolobus alascanus* and longspine thornyhead *Sebastolobus altivelis* are long-lived (Butler et al., 1995; Kline 1996; Kastelle et al., 2000), have extended pelagic larval duration (>1 year) (Dorval et al., 2022), and can reside and feed at OMZ depths of 600–1400 m (Jacobson and Vetter, 1996; Gallo, 2018). Dover sole *Microstomus pacificus* are long-lived (Hunter et al., 1990), and reproduce (Jacobson and Hunter, 1993) and feed on benthic invertebrates inside OMZs (Pearcy and Hancock, 1978; Gallo, 2018). Lastly, the rubynose brotula *Cataetyx rubirostris* is a deep-sea bythitid with wide distribution in the Eastern Pacific and very little known about its basic biology and ecology (Hanke et al., 2015).

The Gulf of California OMZ occurs roughly between 100 and 1300 m depth, with dissolved oxygen concentrations consistently below 22 μ mol kg $^{-1}$, and suboxic conditions (i.e., $O_2 < 5~\mu$ mol kg $^{-1}$) present for more than 500 m of the water column (Zamorano et al., 2007; Hendrickx and Serrano, 2014; Gallo et al., 2020). The southern Gulf of California OMZ sits above the outer continental shelf and the upper slope, with extremely low oxygen concentrations (i.e., $O_2 < 2~\mu$ mol kg $^{-1}$) that excludes most invertebrate species (Zamorano et al., 2007; Hendrickx and Serrano, 2014). A surprising exception is the ophidiid black brotula Cherublema emmelas, a ligooxyphile (i.e., low-oxygen extremophile) fish which thrives at $O_2 \sim 2~\mu$ mol kg $^{-1}$ (Gallo et al., 2019).

About 15,000 km away from the Southern California Bight and the Gulf of California OMZs (Pacific Ocean), the Namibian shelf OMZ (Atlantic Ocean) is part of the Benguela Current Ecosystem and occurs at $\sim 100-300$ m depth. This ecosystem is characterized as one of the most extreme marine habitats in the world due to its perennial hypoxic and anoxic conditions as well as its high hydrogen sulfide concentrations (Hutchings et al., 2009; Salvanes et al., 2011; Currie et al., 2018). In this geologically mature shelf upwelling system, the bearded goby Sufflogobius bibartus exhibits remarkable adaptations to the extreme environmental conditions (Salvanes et al., 2011; Salvanes and Gibbons 2018) and acts as a keystone species, coupling the inhospitable benthic environment with the pelagic system above (Utne-Palm et al., 2010; Currie et al., 2018). Since all these deep-sea species from distant ocean basins reside in OMZs, their otolith chemistries can be influenced by similar environmental (e.g., low oxygen, temperature, pH) and physiological (e.g., feeding on similar prey items, low metabolism) factors (Hüssy et al., 2020).

As a contrast to the deep-sea fishes from OMZs, the giant sea bass *Stereolepis gigas* occupies shallow waters from 3 to 40 m in kelp forests and nearshore rocky reefs of the Northeast Pacific and Gulf of California and is a long lived (~ 76 years), slow-growing and late mature species (Fitch et al., 1971; Hawk and Allen, 2014; Ramírez-Valdez et al., 2021). Therefore, its otolith chemistry is expected to reflect, at least moderately, the water chemistry, oxygen, temperature, and prey items of surface waters (Elsdon and Gillanders, 2002; Walther and Thorrold, 2006; Walther et al., 2010).

The expansion of deep hypoxic zones is expected to alter the range of the distributions and decrease the biodiversity of fishes in these areas (Levin et al., 2009; Stramma et al., 2010, 2012; Salvanes et al., 2015; Gallo and Levin, 2016; Gallo et al., 2020). Overall, demersal fish have higher oxygen requirements than benthic invertebrates (Vaquer-Sunyer and Duarte, 2008), potentially making them more vulnerable to deoxygenation trends. While ecological sampling methods such as trawls or remotely operated vehicles (ROVs) can shed light on community-level patterns, often fine-scale data on how individual fish interact with hypoxic areas is lacking. Identifying tools that can track low oxygen, pH and temperature conditions during fishes' lifetimes can help fill this gap.

1.3. Low oxygen, pH and temperature exposure in OMZ-CMZ fish – looking at otolith chemistry patterns

Chemical analysis of fish otoliths - the calcium carbonate structures that grow periodically throughout the life of a fish - could help to understand fish exposure to hypoxic conditions (Limburg et al., 2011, 2015), low pH (Levin et al., 2015; Paulmier et al., 2011) and cold waters characteristic of OMZs-CMZs (Devereux, 1967; Gerringer et al., 2018). For example, Limburg et al. (2011) reconstructed hypoxia exposure in 1-year-old cod (Gadus morhua) using Mn:Ca ratios, which are potentially bioavailable due to the redox dynamics induced by low-oxygen conditions in nursery sites of the Baltic Sea. Such hypoxia exposure has consequences for cod growth and weight (Limburg and Casini, 2018). Furthermore, Mn:Ca ratios work as a reliable proxy for hypoxia exposure in several other fish species spanning a range of habitat salinities (e.g., Lake Erie, Baltic Sea, and the Gulf of Mexico) (Limburg et al., 2015). Currently, understanding of how OMZs-CMZs environments affect otolith microchemistry remains largely unexplored in open-ocean, deep sea environments.

The elemental composition of otoliths, especially for elements that are redox-sensitive, such as iron (Fe) and manganese (Mn), and which are likely bioavailable inside OMZs (Johnson et al., 1996; Morford and Emerson, 1999; Hopkinson and Barbeau, 2007), have the potential to be used as proxies for hypoxia exposure in deep-water OMZ fish. Temperature is understood to interact with oxygen and CO_2 to set tolerance limits of fish (Pörtner, 2001, 2021) and oxygen isotopes ($\delta^{18}O$) can allow the reconstruction of the thermal history of deep-sea fishes when living in OMZs-CMZs conditions (Gerringer et al., 2018). Therefore, elemental and isotopic analysis can shed light on how hypoxia, hypercapnia (i.e., excess of CO_2 in the blood) and temperature interactively affect deep-water OMZ-dwelling fish.

We hypothesize that the unique biogeochemistry of OMZs-CMZs (i. e., low-oxygen, low-pH, low temperature, and bioavailable elements) will impart distinctive elemental and isotopic signatures upon the otoliths of both long-lived and short-lived fishes. Unlike previous studies, which focused on species from coastal areas, enclosed seas and inland lakes (Limburg et al., 2011, 2015; Altenritter et al., 2018), our analysis is the first to look for elemental proxies of exposure to hypoxia waters in open ocean, deep-sea fishes. The goals of this study are to: (i) compare the otolith chemistry of OMZ-fishes from distant ocean basins, the Northeast Pacific and Southeast Atlantic; (ii) identify trace and minor elements as proxies for exposure to severe hypoxia in fully marine fishes (<20 μmol kg⁻¹ in the Pacific, and <45 μmol kg⁻¹ in the Atlantic); and (iii) reconstruct the thermal history of these species when inhabiting OMZs using oxygen isotope ratios (δ^{18} O). We also explore the use of trace elements as environmental proxies for warm waters during marine heatwaves, such as the Northeast Pacific 2013-2015 warm-water anomaly, referred to as "the Blob" hereafter (Bond et al., 2015). We anticipate that finding new proxies for oxygen, pH and temperature, which act in tandem in deep-sea fishes from OMZs - relatively far from terrigenous influences known to affect the chemistry of otoliths - will be fundamental for understanding how individual fish respond to the continuing deoxygenation, acidification and warming of global oceans.

2. Material and methods

2.1. Regional settings

In the North Pacific Ocean, the elements Ba, Sr, Cu, Zn and Fe have a nutrient-like vertical profile, being depleted in the euphotic zone and enriched with depth (Johnson K.S., 2021; MBARI Periodic Table of Elements in the Ocean). Manganese is particularly interesting in this ocean, as it shows a subsurface maximum ($\sim 500-1500$ m) at low oxygen concentrations (Johnson et al., 1996). In coastal upwelling areas, modern sediments have higher concentrations of organic material often enriched with redox-sensitive trace metals. In the Southern California

Bight, the organic matter and trace elements in seawater derive largely from primary production (upwelling events), natural oil seepage, domestic and industrial discharges, dust deposition, and coastal erosion (Dailey et al., 1993). In the South Atlantic Ocean, off the Namibian shelf, the sediments on the modern shelf are comprised primarily of organic matter, diatomaceous silica and calcium carbonate, and the distributions of Cu, Pb and Zn follow the distribution of organic matter and are enriched in the diatom ooze because of coastal upwelling, while Ba tends to increase towards the slope, away from the diatom ooze (Calvert and Price, 1983). Namibian shelf is also part of the Benguela Upwelling System, where there are high concentrations of dissolved trace metals, including Fe, Co, Mn, Cd, Ni and Cu, and subsurface (200–500 m) fluxes of Fe are higher than surface (0–200 m) fluxes (Liu et al., 2022). Other elements, such as Sr appears relatively constant throughout the water column in the Atlantic Ocean (Johnson K.S., 2021).

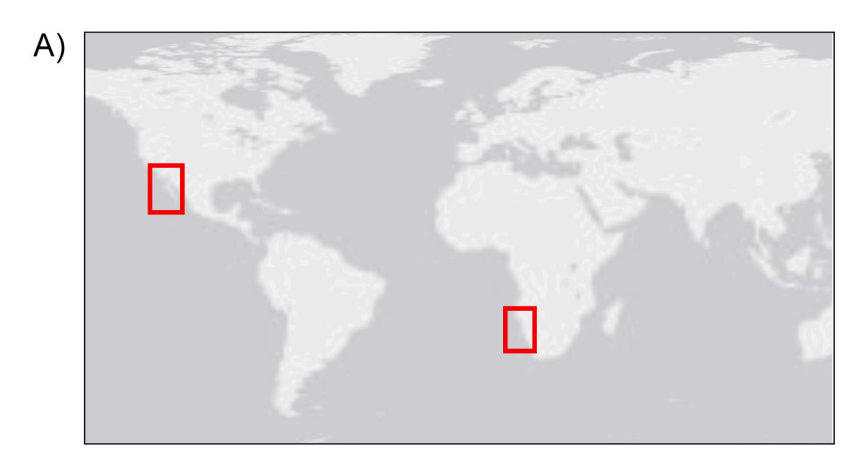
2.2. Fish collection

Deep-sea fishes were obtained from three OMZs; the Southern California Bight (SCB), the Gulf of California (GOC), and the Namibian shelf (Fig. 1). Species collected in SCB included the Dover sole Microstomus pacificus (n = 18), shortspine thornyhead Sebastolobus alascanus (n = 18) 10), longspine thornyhead Sebastolobus altivelis (n = 8), and rubynose brotula Cataetyx rubrirostris (n = 8). These specimens were collected during several research cruises from 2014 to 2016 using otter trawls at depths between 198 and 1280 m along the continental margin (Gallo, 2018). In the GOC, two black brotula Cherublemma emmelas were collected using the Doc Ricketts remotely operated vehicle (ROV) in 2015 at the depth of 793 and 854 m (see Gallo et al., 2020 for sampling details). Off Namibia, bearded goby Sufflogobius bibartus (n = 24) were collected during a cross-shelf cruise in 2012 using demersal and pelagic trawls at depths from 74 to 280 m (see Salvanes et al., 2018 for sampling details). Bearded gobies belong to a family where males exhibit alternative mating tactics: territorial males, which have large body sizes, large sperm duct glands (SDGs) and small testes, and sneaker males, which have small body sizes, with no or small SDGs and large testes (Salvanes et al., 2018). The bearded gobies were defined in each mating tactic by the visual inspection of the gonads and SDGs, following Utne-Palm et al. (2013). As a contrast to conditions experienced in these deep-sea habitats, we also obtained a shallow-water species captured at depths <30 m, the giant sea bass Stereolepis gigas (n=10), which presumably do not live in an oxygen depleted and low pH environment. These specimens were collected off Baja California in 2017 by the commercial and recreational Mexican fishery fleet (Ramírez-Valdez et al., 2021). The selection of deep-sea fish from different OMZs and one shallow-water fish offer interesting contrasts of how distinct oxygen and pH levels affect otolith chemical patterns.

We obtained total length (TL), fork length (FL), total weight (TW), and the right and left sagittae otoliths for each specimen for subsequent chemical analysis. Otolith chemistry, including minor and trace elements and isotopic composition, was quantified using several instruments (Supplementary Table S1).

2.3. Laser ablation inductively coupled mass spectrometry (LA-ICPMS) – minor and trace elements

We quantified minor and trace elements in all fish otoliths except one black brotula individual (n=79) using laser ablation inductively coupled plasma mass spectrometry (LA-ICPMS) at the College of Environmental Science and Forestry at Syracuse, NY. This consisted of a 198-nm laser ablation unit (ESI) connected to an Elan DRc quadrupole mass spectrometer. All otoliths were immersed in epoxy resin Crystal Clear (East Coast Resin), dried for 48 h, and transversally sectioned to about 0.5 mm width. For all the species, except the Dover sole, laser transects spanned from the otolith core to the edge. For the Dover sole otoliths, we selected only the blind-side otoliths as they are in close contact with the



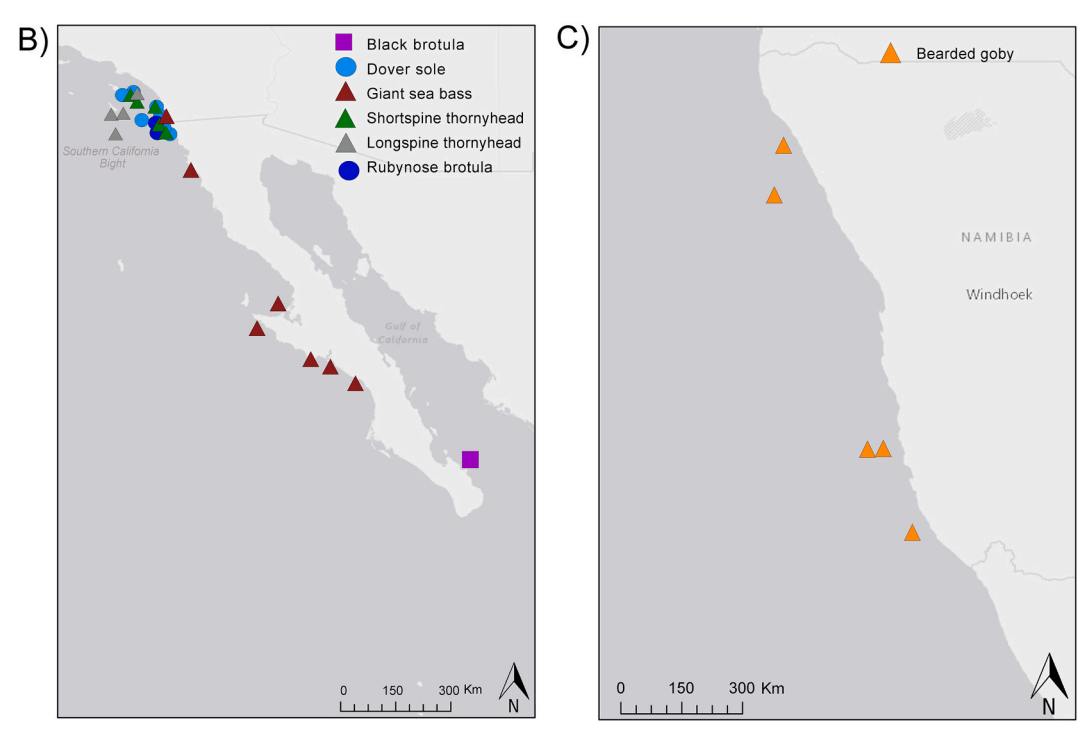


Fig. 1. A) Fish collection sites in the Pacific and Atlantic ocean basins. B) Northeast Pacific: Dover sole, shortspine thornyhead, longspine thornyhead and rubynose brotula (Southern California Bight, U.S.), black brotula (Gulf of California, Mexico), and giant sea bass (west coast of Baja California peninsula, Mexico). B) Southeast Atlantic: Bearded goby (Namibian shelf).

hypoxic sediment, and the laser transects extended from edge to edge, crossing the core (Supplementary Fig. S1). We used a UHP He carrier gas mixed with a flow rate of 800 ml min⁻¹ through the ablation cell. This was mixed with Ar gas flowing at approximately 1 L min⁻¹ to transport the ablated material from the otolith's surface into the plasma of the ICPMS, where the elements were then quantified. Radio Frequency (RF) power was 1200W. ThO/Th was monitored in the Daily Performance Report. The oxide levels were below 4.1% during our runs.

The LA-ICPMS operating parameters for the laser were: 90% power, 10 Hz pulse rate, with an ablation spot size of 35 μm (for smaller otoliths of bearded goby, rubynose brotula and black brotula), 50 μm (for medium size otoliths of Dover sole) and 75 μm (for larger otoliths of thornyheads and giant sea bass), translated across the surface of the otoliths at 5 μm s $^{-1}$ (bearded goby, rubynose brotula, black brotula and Dover sole) or 10 μm s $^{-1}$ (shortspine thornyhead, longspine thornyhead and giant sea bass) scan speed. Transects were pre-ablated to further reduce potential sample contamination. A 40-s washout before and after each sample was run to collect background counts.

We collected data on 10 analytes: lithium (7Li), boron (11B), magnesium (²⁴Mg), calcium (⁴³Ca), manganese (⁵⁵Mn), copper (⁶⁵Cu), zinc (⁶⁶Zn), rubidium (⁸⁵Rb), strontium (⁸⁶Sr), barium (¹³⁸Ba), and lead (²⁰⁸ Pb). An in-house standard of CaCO₃ pellet (Limburg et al., 2015), NIST 612 and MACS-3 (USGS, 2013) were used as standards and were run after every 3-5 otoliths. The trace elements concentrations were analyzed as ratios with 43Ca (Me/Ca, where Me represents a trace element), and data were converted to concentration ratio based on measurements of the NIST 612 standard. We determined a correction factor by dividing measured NIST 612 glass ratios by the mean Me:Ca ratios (ppm) reported in Jochum et al. (2011), (Supplementary Table S2). The measured Me:Ca in our otoliths were then multiplied by the correction factor to standardize measurements and account for daily instrumental drift. Elemental ratios are presented in mmol mol⁻¹ (Sr, Mg and Mn) or μmol mol⁻¹ (Li, B, Cu, Zn, Rb, Ba, and Pb). The mean relative standard deviation (%RSD) for NIST-612 glass during our experiment were: ⁷Li, 17.5%; ¹¹B, 23.3%; ²⁴Mg, 22.1%; ⁴³Ca, 15.5%; ⁵⁵Mn, 13.1%; ⁶⁵Cu, 13.8%; ⁶⁶Zn, 23.3%; ⁸⁵Rb, 17.3%; ⁸⁶Sr, 11.2%; ¹³⁸Ba, 14.5%; ²⁰⁸ Pb, 15.14% (n=16). The precision was based on MACS-3 values and generally ranged from 5% to 10% for ^7Li , ^{24}Mg , ^{43}Ca , ^{55}Mn , ^{86}Sr , ^{138}Ba , and ^{208}Pb , and from 10% to 15% for ^{11}B , ^{65}Cu and ^{66}Zn (n=22).

2.4. Scanning X-ray fluorescence microscopy (SXFM) – 2D elemental maps

We analyzed otolith thin sections by scanning x-ray fluorescence microscopy (SXFM) (n = 15) at the Cornell High Energy Synchrotron Source (CHESS) in Ithaca, NY (Supplementary Table S1). This method is based on the use of high-energy X-rays generated by a synchrotron, as described in Limburg et al. (2011). In summary, a monochromator produces a 16.1 keV X-ray beam that is uniformly focused on a spot from 18 to 100 µm, contingent to the resolution desired and the area of the otolith surface. We collected data on bromine, calcium, strontium, zinc, and iron using a fluorescent X-ray coupled with a Vortex silicon drift detector and added an aluminum foil to lessen calcium counts (a major element in otoliths) and increase sensitivity to the trace elements of interest. The data collected were calibrated based on an in-house standard prepared with compressed otolith powder (Limburg et al., 2011). Spectral analysis was performed by using a Python multichannel analyzer - PvMCA (Solé et al., 2007) and software developed at CHESS to visualize the mass fractions of elements and generate 2D elemental maps. Two-D elemental maps allow us to increase the confidence of elemental patterns observed in the LA-ICPMS, that is, whether a certain element is periodically incorporated within the otolith structure.

We compared the elemental maps of fish collected before and after "the Blob" (Bond et al., 2015) to test for a potential anomalous chemical signal at the edge of the otolith. This event reduced the primary productivity of surface waters, resulting in dramatic changes in the distribution and biomass of several marine species from Alaska to Baja California (Cavole et al., 2016) and potential indirect effects in the deep-sea community. We hypothesize that the Blob's anomalously warm waters at the surface of the ocean reduced primary productivity and subsequently reduced midwater bacterial respiration, leading to increased oxygen concentration in the OMZs.

2.5. Secondary ion mass spectrometry (SIMS) – fish thermal history reconstruction using otolith $\delta^{18}{\rm O}$

In situ $\delta^{18}\mbox{O}$ values were measured from the core of the otolith (larval stage) to the edge (adult stage) using secondary ion mass spectrometry (SIMS) representing at least one individual of each species (Supplementary Table S1). We selected ten otoliths for δ^{18} O isotope analysis, eight of which were also analyzed for trace elements. The trace element profiles of these samples can be found in the Zenodo data repository: 10. 5281/zenodo.7250071. Otoliths were cleaned in methanol and mounted on epoxy resin in aluminum rings together with reference materials for isotope measurements. Samples were polished progressively using silicon carbide grinding papers (600, 800, 1200 grit sizes) to flatten the otolith surface to the µm scale. Polished sections were sonicated in methanol, dried, and gold coated. Otolith sections were examined visually with optical microscopy (Olympus BX51, USA). Pictures were taken at 100, 200 and 400x total magnification using transmitted and reflected light to assist in location of analytical spots for the isotope measurements at the otolith's surface.

Oxygen isotope compositions across the otolith sections were measured using the Cameca IMS-1290-HR ion microprobe at the W.M. Keck Foundation Center for Isotope Geochemistry, UCLA, during two analytical sessions (May-2019, Nov-2019). A Cs $^+$ primary ion beam of $\sim\!2$ nA (Nov-2019) or $\sim\!3$ nA (May-2019) was rastered (5 \times 5 μm^2) over the sample surface (Gaussian beam, ion probe pits of $\sim\!10$ μm). A normal-incidence electron flood gun was used for charge compensation. Following 30 s (May-2019) or 45 s (Nov-2019) of pre-sputtering and subsequent beam centering routines, measurements were made by simultaneously collecting $^{16}O^-$ and $^{18}O^-$ using 2 F cups in the

multicollection detector array. Data were acquired in 6 (Nov-2019) or 10 (May-2019) cycles; counting time for each of the cycles was 10 s. Mass resolving power was set to 2500 for both sessions.

To correct for instrumental mass fractionation (IMF) and to monitor instrumental drift, in-house reference materials (Joplin calcite, $\delta^{18}O=5.8\%$ and optical calcite $\delta^{18}O=11.1\%$ (Shiao et al., 2017), relative to Vienna Standard Mean Ocean Water (VSMOW)) were measured throughout the analytical sessions. The average isotope ratio of the reference material measured throughout that day was used to correct for IMF when no instrumental drift was detected over the course of 24 h. However, in the case where instrumental drift was observed, a standard-unknown-standard bracketing approach was applied. The reproducibility (2 standard deviation) of $\delta^{18}O$ values of reference materials was: Joplin calcite, 0.4‰, over two days; optical calcite, 0.3-2.0%

Measurement errors are given as 2σ and reflect both the in-spot measurement precision (2 standard error) for each analysis and the reproducibility (2 standard deviation) of standard measurements on the analysis day. Data are reported as δ values in parts per thousand (permil; ‰) relative to VSMOW, (Eq. (1)).

$$\delta^{18}O = 1000 * \left(\frac{\frac{18_O}{16_{Oxample}}}{\frac{18_O}{16_{OVSMOW}}} - 1 \right)$$
 (1)

The thermal history for each fish was calculated using equations (2) and (3) stated in Høie et al. (2004). In order to obtain the oxygen isotope ratios in seawater ($\delta^{18}O_{seawater}$), we used the outermost $\delta^{18}O$ values for each otolith, which were assumed to reflect the near-bottom water temperature recorded by CTD-O₂ sensors (Sea-Bird Scientific, Bellevue, WA, USA) at the time of the fish capture. For the giant sea bass, the temperature at the time of fish collection was estimated based on the World Ocean Atlas 2018 database (Supplementary Table S1):

$$\alpha = \frac{\delta^{18} O_{otolith} + 1000}{\delta^{18} O_{seawater} + 1000}$$
 (2)

$$1000 \ln \alpha = 16.75 \left(\frac{1000}{T}\right) - 27.09 \tag{3}$$

(Høie et al., 2004)

The oxygen isotope ratios in seawater ($\delta^{18}O_{seawater}$) were assumed to vary relatively little between shallow and deep OMZ waters and are relatively stable over the short time periods considered here. In the Southern California Bight, for example, $\delta^{18}O$ values are between -0.08 and 0.08% for shallow waters (<200 m) and between -0.01 and 0.02% for deep waters (200 to 1300 m) (Grossman, 1984; Schmidt et al., 1999). Therefore, any larger changes in $\delta^{18}O$ would be mainly attributed to differences in water temperature and not due to oxygen isotope variation in seawater. For example, we know that longspine thornyhead larvae occupy shallower waters ($\sim22-23^{\circ}C$) for an extended pelagic duration before juveniles settle in the OMZ ($\sim4-7^{\circ}C$). This temperature difference would be equivalent to a change of $\sim5\%$ in the $\delta^{18}O$ values, which is much greater than the range of $\delta^{18}O$ values observed for the water masses they occupy ($\pm0.16\%$).

We replicated δ^{18} O values at points at similar distances from the core, and the general trend of increasing δ^{18} O values was consistent for both growth axes. We estimated the age of long-lived species (thornyheads, Dover sole, giant sea bass) by counting annual rings (Hunter et al., 1990; Kline, 1996; Allen and Andrews, 2012) and in short-lived species (bearded goby, rubynose brotula and black brotula) by counting daily growth increments. For the daily growth increments, otolith sections were examined using transmitted light microscopy at 400x magnification and the microscope focus was frequently adjusted to discriminate daily rings from subdaily rings (Campana and Jones, 1992). We then aligned each otolith δ^{18} O analytical spot with its respective calendar date. Data analyses for thermal history

reconstruction were performed using R (R Core Team, 2015) and figures were generated using the package *ggplot2* (Wickham, 2016) and *ggpubr* (Kassambara, 2020).

2.6. Statistical analysis

2.6.1. Principal coordinate analysis

Using a Principal Coordinate Analysis (PCoA), we first tested whether the otolith elemental composition over the lifetime of our fishes (average Me:Ca ratios) enabled discrimination among taxonomic groups (seven species) and/or collection site (Namibian shelf, Southern California Bight and Gulf of California for deep-sea OMZ fishes and surface waters off the Peninsula of Baja California for the giant sea bass). Secondly, we tested whether the otolith elemental composition close to the edge of the otoliths (at 300 µm from the edge for the bearded goby, rubynose brotula and black brotula, at 500 µm from the edge for the thornyheads and Dover soles, and at 1000 µm from the edge for the giant sea bass) and the environmental conditions measured at the time of fish capture (temperature, oxygen, and salinity) enabled discrimination among taxonomic groups and/or collection site. Edge distances were chosen to represent the last 1-2 years of growth and were selected depending on the size of the analytical spot (by LA-ICPMS) and the stability of the elemental material at the edge of each otolith. The variables were standardized using the square root of the average Me:Ca, prior to computing the distance matrix. A dissimilarity matrix was constructed based on the "Gower" method (Gower, 1966). In order to fit Me:Ca ratios onto an ordination plot, we projected the points into vectors that have maximum correlation with corresponding trace elements, using "envfit" function (vegan Package in R). Confidence intervals (CI) of 95% were used to assess the overlap between species or sampling areas and to better visualize group separation or overlap between the species-region combinations; the further the distance between two groups, the greater the dissimilarity.

2.6.2. Flow duration curves to determine the duration of hypoxia events in fish life

We performed an analysis known as "flow duration curve" (fdc) to assess the history of hypoxia recorded in each otolith. This analysis is used in hydrology to calculate the frequency of occurrence of streamflow discharges in a hydrologic time series (Vogel and Fennessey, 1994). The fdc analysis can be adjusted to the elemental time-series data on otolith transects (e.g., obtained with LA-ICPMS) to estimate fish exposure to hypoxia based on chosen Mn:Ca thresholds (Limburg et al., 2015). We calculated the concentration exceedance curves (cumulative distribution functions) of otolith Mn:Ca ratios for all fishes using the "fdc" function (hydroTSM Package in R). The "fdc" allowed us to estimate the percentage of data (i.e., the time-series for Mn:Ca in otolith transects) that exceed a certain threshold for Mn:Ca, which is assumed to correspond to the duration of hypoxia exposure experienced by a fish in its natural environment. Two values were tested to represent hypoxia thresholds; 0.01 mmol mol⁻¹ Mn:Ca, based on the hypoxia threshold used for coastal species (Limburg et al., 2015), and 0.0001 mmol mol-1 Mn:Ca, considering Mn concentrations in OMZ waters, which is \sim 1, 000-10,000 below those observed in coastal dead zones such as the Baltic Sea. We also chose our hypoxia thresholds based on the biology of the deep-sea fishes. Dover sole and shortspine thornyhead inhabit non-hypoxic shallow waters on the shelf before migrating downslope into the OMZ as they get older (Hunter et al., 1990; Jacobson and Hunter, 1993; Jacobson and Vetter 1996). This contrasts to longspine thornyhead, which settle directly into the OMZ (Jacobson and Vetter, 1996; Love et al., 2002). As the adults of the deep-sea fishes analyzed herein have centers of abundance within OMZs (Gallo et al., 2016), they are exposed to severely hypoxic conditions during most of their lifetimes, and therefore, our chosen hypoxia thresholds should be able to reflect these hypoxic patterns.

2.6.3. Kruskal-Wallis test

We performed a non-parametric Kruskal-Wallis test by rank since most of our elemental data (Me:Ca) were not normally distributed (Supplementary Fig. S2). We tested whether there was a significant difference in average Me:Ca ratios among deep-sea fishes from the Southern California Bight OMZ (Dover sole, shortspine thornyhead, longspine thornyhead, rubynose brotula), the deep-sea bearded goby from the Namibian shelf OMZ, and the shallow-water giant sea bass off Pacific Baja California waters. We focused our analysis on the elements that were significantly different between the deep-sea fishes and the shallow-water giant sea bass, but we also presented results for the elements that were most similar between the groups (Supplementary Fig. S3).

2.6.4. Regression analysis of Mn:Ca ratios and fish size/age

To test for the potential influence of fish size or age on manganese incorporation into otoliths, we fitted a linear model to predict Mn:Ca (mmol mol^{-1}) average lifetime ratios from fish size (mm) and/or estimated age (years) for each species (bearded goby, Dover sole, shortspine thornyhead, longspine thornyhead, rubynose brotula and giant sea bass):

Mn:Ca ~ fish size/age * Species

We included an interaction term (*), which is equivalent to dividing the data into species and fitting a linear model for each species group separately and performed linear regressions using the function "lm" in R. Significance levels were assessed using alpha <0.05 (Supplementary Fig. S4).

2.6.5. Temporal analysis of Mn:Ca ratios

To examine potential temporal patterns in recent Mn:Ca ratios (i.e., otolith edge), we analyzed the deep-sea fishes from SCB OMZ by collection year (2014, 2015 and 2016) and the bearded goby from Namibia OMZ and the giant sea bass off Baja California per month of collection, as these fish were collected in a single year in 2012 and 2017, respectively. To test whether the averages of Mn:Ca ratios are significantly different over time, we performed a one-way analysis of variance (Anova) for each species using the function "aov" in R, where:

Mn:Ca ~ time (year/month)

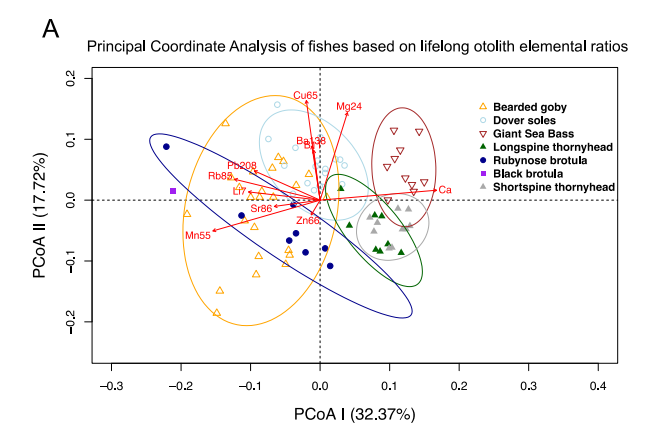
Overall, manganese ratios were relatively stable over time for all species (p > 0.05), and therefore no further analysis was conducted to separate temporal and spatial influences on elemental patterns (Supplementary Fig. S5).

3. Results

3.1. Similar patterns of minor and trace elements in otoliths from Oxygen Minimum Zones (LA-ICPMS)

Deep-sea fish species from Oxygen Minimum Zones (OMZs) in Southern California Bight (Dover sole, thornyheads, rubynose brotula), Namibia (bearded goby) and Gulf of California (black brotula) exhibited similar lifelong otolith microchemistry (Fig. 2A). These species were living under hypoxic (<60 μ mol kg $^{-1}$ in the Pacific, and <90 μ mol kg $^{-1}$ in the Atlantic) and severely hypoxic conditions (<20 μ mol kg $^{-1}$ in the Pacific, and <45 μ mol kg $^{-1}$ in the Atlantic) during most of their lifetimes (Supplementary Table S1). For example, the bearded goby, Dover sole and rubynose brotula overlapped their otolith microchemistries (95% confidence level) (Fig. 2A) and were correlated with the manganese (Mn 55) vector. Strontium and manganese were generally higher in OMZ fish (irrespective of location) than in the giant sea bass from shallower, better oxygenated waters in the Northeastern Pacific (Fig. 3A and B).

When we incorporate the environmental factors (e.g., temperature, oxygen, and salinity) obtained at the time of fish collection, and consider



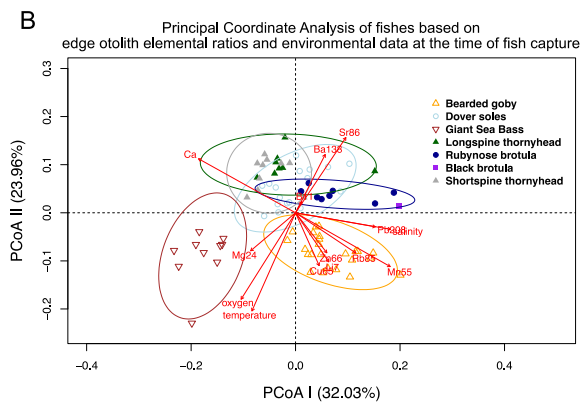


Fig. 2. Principal Coordinate Analysis (PCoA) of otolith microchemistry data for deep-sea fishes (bearded goby, Dover Sole, thornyheads, rubynose brotula, black brotula), and shallow-water fish (giant sea bass). Each symbol represents one fish. Environmental vectors (red arrows) are included to indicate: (A) relationships between trace element ratios (Me:Ca) averaged over the lifetime of the fish (i.e., core-to-edge otolith transect) and PCoA axes, and (B) relationships between trace element ratios (Me:Ca) at the edge of the otoliths and environmental factors at the time of fish collection (e.g., temperature, salinity and oxygen) and PCoA axes.

only the chemistry incorporated at the edge of the otoliths, we obtained similar results (Fig. 2B), but observe a larger separation between the demersal fish from the SCB OMZ and the bearded gobies from the Namibian OMZ, driven mainly by differences in temperature and oxygen at the time of collection (i.e., longer red arrows in Fig. 2B). The shallow-water giant sea bass is distinct from all the other species (Fig. 2A and B). This species does not live in perennial oxygen-depleted areas, and usually experiences oxygen concentrations above 200 μ mol mol⁻¹ (Table 1), although hypoxic events might occur within areas shallower than 50 m in certain years, particularly associated with red tides (Clements et al., 2020). Magnesium and copper ratios tend to be higher for the giant sea bass otoliths than for the deeper water fish from the SCB, the GOC, and the Namibian shelf OMZs (Fig. 3 C, H).

3.2. Higher hypoxia exposure in deep-sea fishes from Oxygen Minimum Zones (LA-ICPMS and SXFM)

Flow duration curves (fdc) were used to calculate the duration of hypoxia exposure based on the Mn:Ca otolith transects obtained with the LA-ICPMS. Using a hypoxia threshold of 0.01 mmol mol⁻¹ Mn:Ca (Fig. 4) (similar to the hypoxic thresholds used for coastal species by Limburg et al., 2015), we found that only the bearded gobies from Namibia and the black brotula from the GOC have experienced severe hypoxia exposure (Table 2). Using a lower hypoxia threshold of 0.0001 mmol mol⁻¹ Mn:Ca (Fig. 4), we observed that most of the deep-sea fishes spend most of their lives under hypoxic conditions (Table 2). Conversely, it appears that the giant sea basses we sampled experienced hypoxia only during at about 22% of their lifetimes. When examining the duration of hypoxia exposure among individuals, the fish that appears to have experienced the most prolonged exposure to hypoxia were the black brotula from the GOC (oxygen concentration = 1.7 μ mol kg⁻¹; Gallo et al., 2019), and two female bearded gobies from the northern stations of Namibia (oxygen concentration = $23.56 \,\mu\text{mol kg}^{-1}$). These females are noted in Fig. 3A as outliers for average Mn:Ca ratios (~ 0.04 mmol mol⁻¹).

The giant sea bass had lower otolith Mn:Ca and Sr:Ca and higher Cu: Ca and Mg:Ca ratios than the OMZ-fishes from the Southern California Bight and the Namibian shelf (Wilcoxon test p < 0.005) (Fig. 5). Fishes from the Southern California Bight OMZ also exhibited lower otolith Mn: Ca than the bearded gobies from Namibian OMZ (Wilcoxon test p < 0.005). The other elemental ratios were relatively similar among groups,

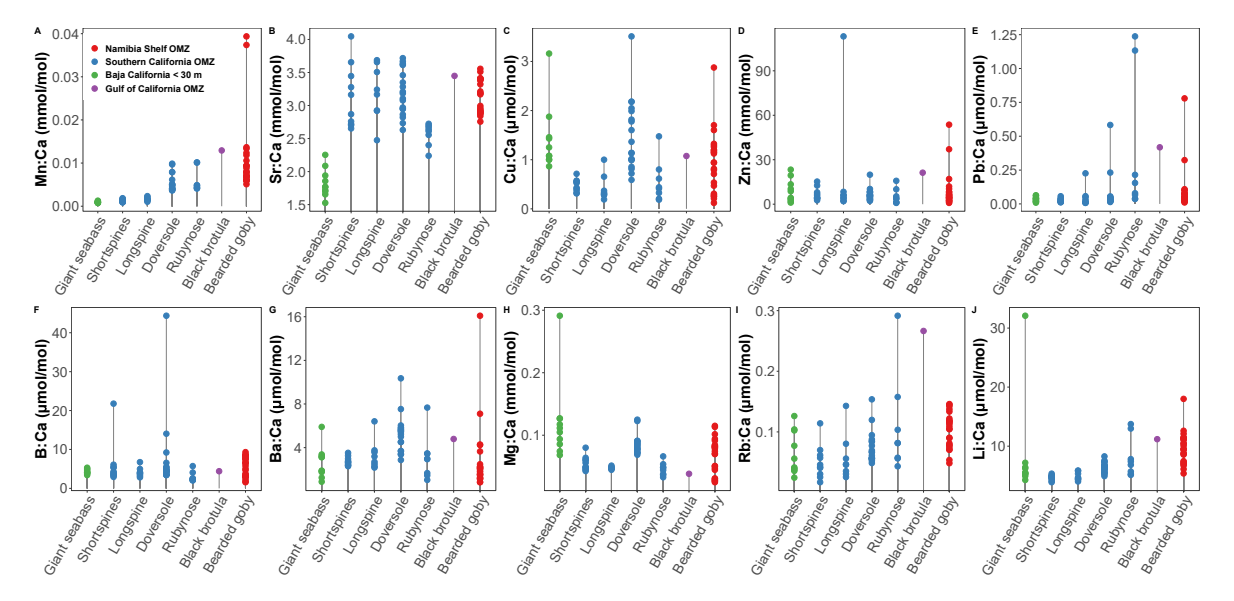


Fig. 3. Elemental ratios for marine fish species. Each dot represents the average elemental ratio (Me:Ca) over the fish lifetime (i.e., core-to-edge otolith transect). The blue dots correspond to fishes from the Southern California Bight OMZ, the purple dot is one black brotula specimen collected with a ROV from the Gulf of California OMZ, the red dots are the bearded gobies off the Namibian shelf OMZ, and the green dots are the shallow giant sea bass off the Baja California Peninsula.

Table 1
Fish (n = 79) used for the quantification of trace and minor elements of otoliths using LA-ICPMS and the respective environmental data (depth, temperature, oxygen, and salinity) obtained from a CTD-O at the time of fish collection. Environmental data for the giant sea bass samples were obtained using the World Ocean Atlas 2018 database.

Common name	Scientific name	n	Year of collection	Location	Depth (m)	T (°C)	O ₂ (μmol kg ⁻¹)	Salinity (psu)
Longspine thornyhead	Sebastolobus altivelis	8	2014–2015	Southern California Bight OMZ	475–1280	4.09-6.71	8.17–19.28	34.17–34.46
Shortspine thornyhead	Sebastolobus alascanus	10	2014–2015	Southern California Bight OMZ	339–878	4.41-8.11	7.38–44.39	34.15–34.45
Dover sole	Microstomus pacificus	18	2014–2016	Southern California Bight OMZ	198–1115	4.22- 10.17	8.17–92	34–34.46
Rubynose brotula	Cataetyx rubirostris	8	2014	Southern California Bight OMZ	607-705	5.39-5.43	8.29-8.43	34.39
Black brotula	Cherublemma emmelas	1	2015	Gulf of California OMZ	793	6.02	1.73	34.54
Bearded goby	Sufflogobius bibartus	24	2012	Namibia shelf OMZ	74–280	9.73- 13.56	21.75–150.96	34.76-35.32
Giant sea bass	Stereolepis gigas	10	2017	Pacific coast of Baja California – shallow waters <30 m depth	30	13.70- 20.46	65.29–255.08	33.34-33.78



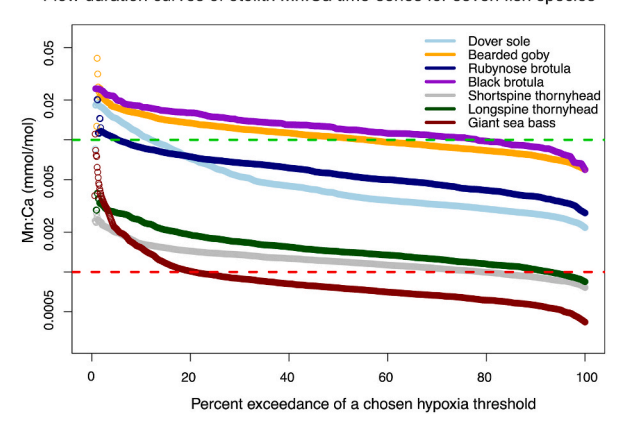


Fig. 4. Mn:Ca (mmol mol⁻¹) exceedance curves for Dover sole, bearded goby, rubynose brotula, black brotula, shortspine thornyhead, longspine thornyhead (deep-sea fish from Oxygen Minimum Zones) and giant sea bass (shallow-water fish) above 0.01 mmol mol⁻¹ Mn:Ca ratios (dotted green line) and above 0.0001 mmol mol⁻¹ Mn:Ca ratios (dotted red lines) hypoxia thresholds. Exceedance curves are calculated as measurements of Mn:Ca above a chosen Mn:Ca threshold, divided by the core-to-edge otolith transects.

Table 2Maximum Mn:Ca ratios (mmol mol⁻¹) and the estimated duration of hypoxia for deep-sea fishes from Southern California, Gulf of California and Namibia OMZs and the shallow-water giant sea bass off Baja California Peninsula. The duration of hypoxia is defined as the percentage of time the Mn:Ca ratios along the otolith transect exceeded a chosen hypoxia threshold, meaning that these individuals were exposed to hypoxic conditions in their environment.

Species	n	max Mn:	Duration of hypoxia						
		Ca	Hypoxia threshold (> 0.01 mmol mol ⁻¹)	Hypoxia threshold (> 0.0001 mmol mol ⁻¹)					
Longspine thornyhead	8	0.00234	0%	87.37%					
Shortspine thornyhead	10	0.00185	0%	63.11%					
Dover sole	18	0.00987	8.86%	100%					
Rubynose brotula	8	0.0101	10.70%	100%					
Black brotula	1	0.0129	77.77%	100%					
Bearded goby	24	0.0394	31.44%	100%					
Giant sea bass	10	0.0012	0.07%	22.02%					

except for Ba:Ca, which was higher for SCB deep-sea fishes, and Rb:Ca and Li:Ca, which were higher for bearded gobies from the Namibian shelf OMZ (Supplementary Fig. S3).

Potentially related with fish exposure to severe hypoxic conditions, two-D elemental maps of Fe:Ca were measured using SFXM and were higher outside the core region of longspine thornyheads (LST; Fig. 6), corresponding to adult stages after settlement in deep waters (~ 600 m), although very low concentrations for this element make visualization challenging. Out of eight bearded gobies analyzed, one individual (#3269), a territorial male (identified by its morphological features) collected at 280 m depth and 23.53 $\mu \rm mol~kg^{-1}$ in Namibian waters, showed higher Fe:Ca and Zn:Ca at the core of the otolith (Fig. 6). The longspine thornyheads, shortspine thornyheads, Dover soles and the one black brotula from the Pacific Ocean also presented well-defined Zn:Ca rings in their otoliths, suggesting this element is incorporated periodically into the otolith crystal structure.

3.3. Fish size and age are not correlated to Mn:Ca ratios in otoliths (LA-ICPMS)

Average lifetime manganese to calcium (Mn:Ca) did not increase with fish size (mm) or age (year) for any of the deep-sea OMZ fishes or the shallow-water giant sea bass (Supplementary Fig. S4), suggesting that this element might respond more to environmental variations than endogenous controls for the species analyzed.

3.4. Potential effects of the "blob" warm-water anomaly in the otoliths of deep-sea fishes (SXFM)

Two-D elemental maps allowed us to observe fine-scale patterns in environmental conditions throughout the lifetime of deep-sea fish, including potential changes during "the Blob" (Fig. 6). We observed subtle differences at the edges of the otoliths of the longspine thornyhead, shortspine thornyhead and Dover sole collected in July 2014 ("Pre-blob LST 705 m"; "Pre-blob SST 705 m"; "Pre-blob Dover sole 698 m") compared to specimens collected in September 2015 ("Post-blob LST 703 m"; "Post-blob SST 703"; "Post-blob Dover sole 703 m") (Fig. 6). For example, Br:Ca and Zn:Ca tend to be higher at the edge of the otoliths collected after "the Blob".

Longspines collected before and after the "Blob" showed high Sr:Ca after the settlement stage (otolith core), suggesting that adults consistently live in high salinity and deep waters, regardless of this phenomenon. Based on Sr:Ca ratios, the shortspine thornyhead collected after the "Blob" was potentially living deeper than the individual collected before the "Blob", while the opposite pattern was observed for the Dover soles (Fig. 6), suggesting individual variations in behavior and vertical ontogenetic patterns.

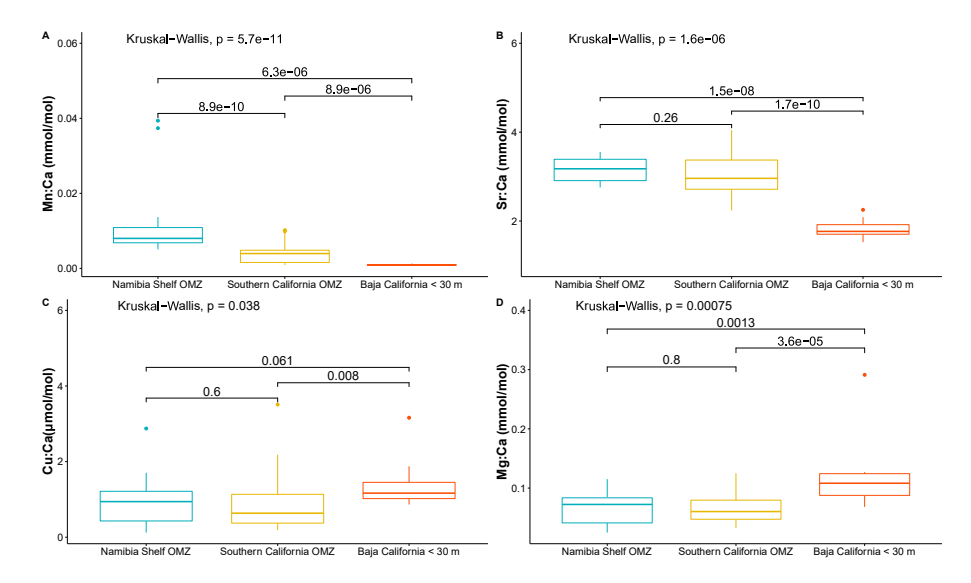


Fig. 5. Boxplot of a Kruskal-Wallis test of Me:Ca (mmol mol^{-1} or μ mol mol^{-1}) otolith ratios between the bearded gobies from the Namibian shelf OMZ, demersal species from the Southern California Bight OMZ and the giant sea bass from surface waters off the peninsula of Baja California (<30 m deep). A global Kruskal-Wallis p-value is provided at the top of the graphic, as well as pairwise comparisons p-values based on the Wilcoxon test.

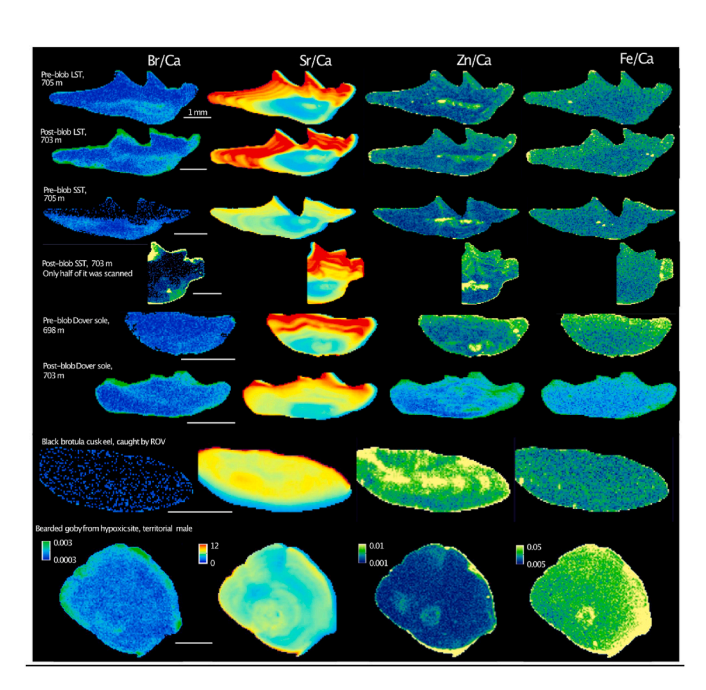


Fig. 6. Two-D elemental maps of otolith sections from OMZ-dwelling fishes analyzed by SXFM. Bromine to calcium (Br/Ca), strontium to calcium (Sr/Ca), zinc to calcium (Zn/Ca) and iron to calcium (Fe/Ca) maps are presented for a shortspine thornyhead (SST), longspine thornyhead (LST) and Dover sole collected in the Southern California Bight before and after the Northeast Pacific 2013–2015 "Blob", for a black brotula collected in the Gulf of California and for a bearded goby collected on the Namibian shelf. (*color should be used).

3.5. Deep-sea fishes live in cold waters characteristic of Oxygen Minimum Zones (SIMS)

The thermal history reconstruction based on otolith $\delta^{18}O$ values allowed us to: (1) assess whether temperature drove the elemental composition patterns of fish otoliths from the NE Pacific and SE Atlantic OMZs (Fig. 2); (2) infer at which life stages, and for how long, the deepsea fishes were living at cooler temperature ranges typical of the relevant OMZs; and (3) examine patterns of ontogenetic migration for the deep-sea species and the shallow-water giant sea bass.

Overall, the relative changes in seawater temperatures calculated across each fish's otolith (representing lifetime archives) were sufficiently pronounced to produce distinct otolith δ^{18} O signatures. The δ^{18} O values ranged from 28.4 to 36.3% relative to VSMOW for all deep-sea fish, and from 27.9 to 31.8% for the giant sea bass (Table 3). The standard errors (20) of individual point measurements ranged from ± 0.31 to \pm 0.94‰. The highest values for otolith $\delta^{18}O$, which correspond to lower habitat temperatures and OMZs-CMZs residency, were consistently observed for all deep-sea fish, except for rubynose brotula (Fig. 7). Fishes from OMZs generally exhibited otolith δ^{18} O patterns that suggest a pelagic larval phase in warmer, shallower waters, followed by a progressive ontogenetic vertical migration into colder, deeper waters. For example, the longspine thornyhead may have experienced high temperatures at the larval stage (~ 23 °C), before settling at greater depths in colder waters (\sim 5 $^{\circ}$ C), where it remained for the rest of its life (Fig. 7A). This pattern was less prominent for the Dover sole, rubynose brotula and black brotula, since they seem to be moving more frequently in the water column at younger ages, before being consistently exposed to cooler conditions as adults within the OMZ (Fig. 7B, D-F). The shortspine thornyhead showed a thermal history that suggests cyclical movements up and down the continental margin throughout its relatively long ontogeny (40 years) (Fig. 7C, Table 3). Off the Namibian shelf, we analyzed two bearded goby otoliths that exhibited markedly distinct habitat temperature trends. The bearded goby #3081 was a sneaker male that underwent a large temperature variation of almost 18 °C (Fig. 7G), whereas the bearded goby #3044, a female, appears to have been exposed to much smaller temperature variation (~10 °C) (Fig. 7H). The thermal history reconstruction for two giant sea bass specimens (Fig. 7I and J) revealed a similar trend to that of the shortspine thornyhead of recurrent changes in depth, although the giant sea bass do not appear to live in the deep OMZs of the Southern California Bight ($\sim 400-1200 \text{ m depth}$).

4. Discussion

4.1. Similar elemental composition in fish otoliths from distant OMZs

Our results suggest that fishes that live in OMZs from the NE Pacific and SE Atlantic oceans experience similar environmental and physiological conditions that are reflected in distinctive minor and trace elemental composition in their otoliths (Fig. 2). It is possible that the biogeochemistry of the OMZs-CMZs waters modulates the amount of

Table 3

Thermal history reconstruction for 10 marine fish individuals. Depth (m), temperature (°C), dissolved oxygen (μ mol kg⁻¹) and salinity (psu) at the time of collection are provided for each specimen. δ^{18} O values (% vs. VSMOW) for seawater were estimated based on outermost spot and temperature at the time of fish collection. Lengths (L, cm) are standard length for shortspine and longspine thornyheads, Dover soles, rubynose brotula and black brotula and total length for bearded gobies and giant sea bass. Total weight (TW, g) and age in years or days are provided for each individual. Spots are the number of isotope values measured along the otolith transect. The range of δ^{18} O values (% vs. VSMOW) recorded in the otoliths and their respective estimated lifetime temperatures are provided.

Species	Fish ID	Depth (m)	T (°C)	O ₂ (μmol kg ⁻ 1)	Salinity	$\delta^{18}O_{sw}$	L (cm)	TW (g)	Age	Spots (n)	$\delta^{18}O$ otolith	Estimated T (°C)
Longspine thornyhead	#951	951	4.46	12.30	34.34	-1.06	20.2	217.69	34 yrs	31	28.4–33.3	1.5–25.0
Shortspine thornyhead	#703	703	5.59	9.76	34.36	0.89	31.10	591	40 yrs	18	32.5–35.4	1.3–14.5
Dover sole	#1116	1115	4.22	11.05	34.47	0.39	30.7	471.76	30 yrs	14	31.8-34.2	4.2-15.5
Rubynose brotula	#705	705	5.39	8.30	34.39	2.65	10.9	7.24	13 yrs	13	32.7-36.3	5.3-22.3
Black brotula	#732	793	6.02	1.74	34.54	0.33	15.1	14.38	272 days	15	31.4–34.1	4.4–16.8
Black brotula	#737	854	5.13	4.12	34.52	0.94	20.1	52.59	330 days	13	32.1–34.8	4.0–16.4
Bearded goby	#3081	280	10.93	23.53	34.97	-0.72	8.80	5.3	2 yrs	21	28.5-32.1	8.3-26.2
Bearded goby	#3044	280	10.93	23.53	34.97	-0.01	10.2	3.8	3 yrs	14	30.9-33.2	7.0-17.5
Giant sea bass	#170506	30	16.65	239.90	33.36	-0.96	172	140000	41 yrs	41	28.0-31.8	8.7-27.6
Giant sea bass	#170606	30	13.82	224.51	33.78	-1.77	195	117000	44 yrs	37	27.9–31.2	7.7–23.4

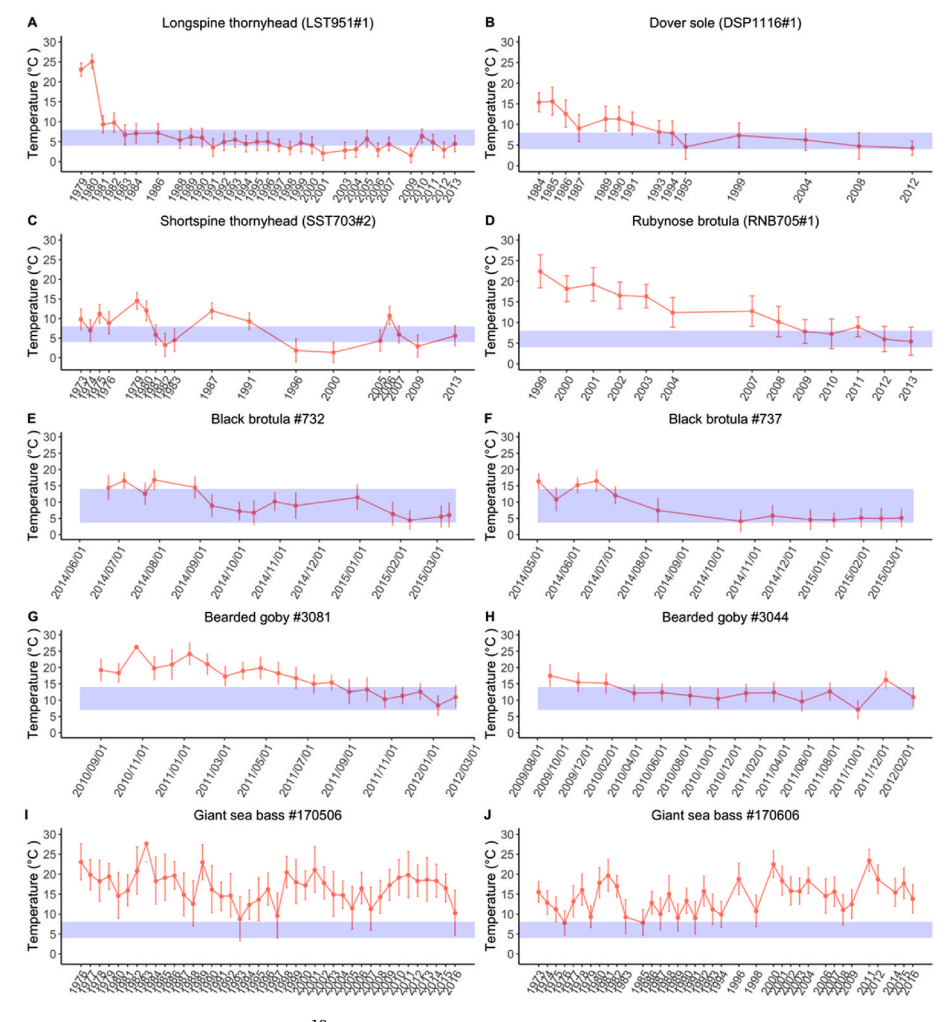


Fig. 7. Thermal history reconstruction for fishes based on δ^{18} O values from otoliths (red line). For all fishes, SIMS spots were aligned with the corresponding calendar date estimated at an annual or daily resolution. Blue rectangles indicate the temperature ranges characteristic of OMZs-CMZs in each ecosystem. The giant sea bass is a shallow-water species, such that its estimated temperature is consistently outside the OMZ temperature range (blue rectangles).

minor and trace elements dissolved in seawater as well as fishes' physiological responses to extreme hypoxia. Indeed, the California and Benguela Current Ecosystems are two of the four major Eastern Boundary Upwelling Systems (EBUS) in the world (Mackas et al., 2006;

Chavez and Messié, 2009). EBUS are very productive systems (Carr, 2002), with OMZs-CMZs characterized by similar biogeochemical mechanisms (remineralization processes leading to high DIC and low O₂) (Paulmier et al., 2011) and by similar redox mechanisms that

regulate the bioavailability of metals such as iron, copper, and manganese (Morford and Emerson, 1999; Hopkinson and Barbeau, 2007; Liu et al., 2022). Indeed, strontium, barium, iron, and zinc have a nutrient-like profile in the Pacific Ocean (Johnson K.S., 2021; MBARI Periodic Table of Elements in the Ocean) and this trend was also observed in the otoliths of long-lived deep-sea fishes (Fig. 6; Supplementary Fig. S1). Iron is enriched at subsurface waters (200–500 m) in the Benguela Current Ecosystem, and this element was detected in the otolith of a bearded goby (Fig. 6).

Patterns of lifetime elemental composition in otoliths (i.e., core-toedge) were markedly similar among the Dover sole Microstomus pacificus from the Southern California Bight (SCB), the bearded goby Sufflogobius bibartus from the Namibian shelf and the black brotula Cherublemma emmelas from the Gulf of California (Fig. 2A), despite having different life-history traits. Off the coast of California, Dover sole can grow to ~ 50 cm in length, live up to 58 years (estimated), and reproduce at 640-1000 m (Hunter et al., 1990). The bearded gobies are endemic to west Africa (South Africa to southern Angola), occur from the shore to 400 m depth (Staby and Krakstad, 2006), are short-lived (6 years) (Melo and Le Clus, 2005), and undergo diel vertical migrations between the hypoxic and anoxic seabed and shallower, more oxygen-rich midwaters (Utne-Palm et al., 2010). The abundance of bearded gobies seems to increase with the decrease in oxygen concentration (Salvanes et al., 2015). The black brotula analyzed herein was caught in the lowest oxygen concentrations measured in this study (O2 = 1.73 μmol kg⁻¹), and individuals were frequently observed with their heads buried in the sediment (Gallo et al., 2019). Black brotulas are present in high densities in the southern Gulf of California (Zamorano et al., 2014), are short-lived (i.e., 5 years) (Morales-Azpeitia et al., 2018), and are dominant members of the demersal fish community under the most hypoxic conditions (Gallo et al., 2020). The trace elements measured in the black brotula otolith for Cu, Zn, Pb, Mn seem to correspond to the concentrations observed in the tissues of myctophid fish from the GOC (Figueiredo et al., 2020), suggesting similar physiological, ecological, and environmental factors in the mesopelagic layer.

Notably, the bearded gobies on the Namibian shelf, and the Dover soles from Southern California Bight, appear to associate with microbial mats on the ocean floor. For the bearded goby, fatty acid and stable isotope signatures in tissues have revealed that the diatom- and bacteriarich sulphidic sediments play an important role in their diet (Van der Bank et al., 2011). In the California Current Ecosystem, frequent remotely operated vehicle (ROV) observations of Dover sole resting on microbial mats at methane seeps at depths ~ 720–1020 m (Grupe et al., 2015; Levin et al., 2016) indicate that they can withstand suboptimal conditions and potentially feed on benthic invertebrates adapted to these microhabitats. Although the mechanisms driving the common elemental fingerprints are unclear, the close contact of Dover sole and bearded goby with the substrate might influence their otolith microchemistry similarly.

The shortspine thornyhead *Sebastolobus alascanus* and longspine thornyhead *Sebastolobus altivelis* displayed similar elemental signatures to one another (Fig. 2A and B). These species are sympatric as adults in the northeast Pacific and overlap at depths of 600 to 1000 m. *Sebastolobus* species have long lifespans, estimated to be over 100 years in the shortspine thornyhead and over 45 years in the longspine thornyheads (Butler et al., 1995; Kline, 1996; Kastelle et al., 2000). Lastly, the rubynose brotula, *Cataetyx rubirostris*, a small deep-sea bythitid whose population dynamics and ecological role have remained relatively unknown in the North Pacific Ocean (Nielsen et al., 1999; Gibbs, 1999), presented similar otolith chemistries to the bearded gobies from the South Atlantic Ocean (Fig. 2A).

All the deep-sea fishes had otolith chemistry significantly different from the giant sea bass, *Stereolepis gigas*. The giant sea bass occurs within relatively shallow waters up to \sim 30 deep (Ramírez-Valdez et al., 2021). At this depth, oxygen and pH conditions vary, but values are consistently higher than those found for our deep OMZ fishes (Table 1). Despite the

similarity of otolith chemistry among fishes from two EBUS and the one black brotula from the Gulf of California OMZ (Fig. 2), much uncertainty remains in understanding these complex ecosystems. Both the California and the Benguela EBUS have marine sediments produced by a reduced dilution of planktonic and skeletal materials, since the coastal region is arid or semi-arid and perennial rivers are few or absent, and by the deposition of organic material with a short transport time from surface waters to the seabed (Calvert and Price, 1983). Of note, the bioavailability of trace elements that can be incorporated into benthic organisms depends not only on the presence of the trace elements in the seabed, but also on the physicochemical characteristics of the near-bottom water and redox condition of the depositional environment. Water oxygen content, for example, can change the oxidation state of metals and release them back into the water column (Abshire et al., 2020; Bennett and Canfield, 2020). Furthermore, physiological aspects (e.g., feeding, gas exchange, growth, reproduction, and metabolism) are important factors influencing the chemistry and morphology of otoliths (Kalish 1989; Esbaugh et al., 2012 Sturrock et al., 2014, 2015; Kwan and Tresguerres, 2022), and could be responsible for unique elemental patterns found in OMZ-CMZs, particularly for those elements that bind into the otolith organic matrix, such as P, Cu, and Zn (Hüssy et al., 2020) or elements that can biomagnify in tissues, such Cu, Zn, Cd and Pb (Figueiredo et al., 2020).

Following this rationale, we hypothesize that the unique biogeochemistry of OMZs, along with similar physiological constraints related to low oxygen, pH and temperature conditions, have jointly played an important role in the final uptake of elements in these deep-sea fish otoliths.

4.2. Manganese as a proxy for hypoxia in fish. Does it work for deep-sea species?

In the search for suitable elemental proxies for hypoxia exposure in fish, manganese is currently the most promising (Limburg et al., 2011, 2015). Manganese is bioavailable from the substrate to the water column under low oxygen conditions and has been found to occur at relatively high concentrations in the Baltic Sea cod Gadus morhua, Baltic flounder Platichthys flesus, winter flounder Pseudopleuronectes americana, alewife Alosa pseudoharengus, Atlantic croaker Micropogonias undulatus, and yellow perch Perca flavescens (Limburg et al., 2011, 2015; Altenritter et al., 2018; Limburg and Casini, 2018). Compared to these estuarine and coastal species of the Atlantic Ocean, we only detected high ratios of manganese in the otoliths of the bearded gobies (Namibia) and the one black brotula (Gulf of California OMZ) whereas all other deep-sea fishes from Southern California OMZ had much lower average Mn:Ca in their otoliths (Supplementary Table S3). These lower than expected Mn:Ca values may be due to the lower concentrations of manganese in the Southern California Bight. At the northern range of the SCB OMZ (35°N) between 400 and 1000 m, manganese concentrations are extremely low at approximately 1.25 nM, which is around 10,000 times lower than in the Baltic Sea (Johnson et al., 1992). Therefore, it is important to take into consideration the background concentrations of trace elements in coastal ecosystems and enclosed seas vs. open OMZs. In our case, this is especially relevant for SCB, where fishes were collected between 200 and 1280 m depth, relatively far from terrigenous input of Mn, in comparison with shallow coastal bays, estuaries and lagoons (Johnson et al., 1992; van Hulten et al., 2016). Despite low Mn:Ca ratios observed for all fishes in this study, all OMZ specimens still exhibited higher Mn:Ca than the shallower giant sea bass (Figs. 3A and 5), which is an unexpected result, since the concentration of manganese in surface waters off California (2-2.5 nM), where the giant sea bass reside, is twice as much as the waters within its OMZ (1-1.25 nM) (Johnson et al., 1992). This suggests that both elemental bioavailability and background concentrations must be considered when interpreting otolith patterns.

In order to detect exposure to hypoxia in deep-sea species, the value chosen for the Mn:Ca hypoxia threshold may need to be lower than that

used for nearshore coastal, estuarine and enclosed sea species (e.g., Baltic Sea, Gulf of Mexico). Use of both of our low (0.0001 mmol mol $^{-1}$) and higher (0.01 mmol mol $^{-1}$) Mn:Ca thresholds for hypoxia suggested that black brotula, bearded gobies, rubynose brotulas and Dover soles are the species experiencing the most hypoxic conditions in their respective deep-sea environments (Fig. 4). For the bearded gobies, four females experienced hypoxia during most of their lifetimes. These females were captured at 23.56 μ mol kg $^{-1}$ of O2, indicating that they may be particularly exposed to hypoxia in Namibian waters. This seems to contradict previous behavioral studies that indicate that females are "free" to undertake diel vertical migrations and thus visit more oxygenated upper waters than territorial males (Skrypzeck et al., 2014; Salvanes et al., 2018).

4.3. Other elements as proxies for hypoxia in fish. Does it work for deepsea fish?

Other elements analyzed by LA-ICPMS that follow a similar trend to that of manganese were strontium and barium (Figs. 3–5; Supplementary Figs. S1–S3). Barium has a nutrient-like profile distribution in the ocean, being scavenged and of low concentration in surface waters and exported and enriched in deep and cold waters, rich in nutrients (Bruland and Lohan, 2004), and therefore, might exist in higher concentrations within the OMZs than in surface waters. Strontium correlates with salinity and tends to be incorporated into otoliths in proportion to ambient concentrations. In the deep sea, cold and high salinity waters sink, and might explain the significantly higher concentrations of this element in our deep-sea OMZ fishes.

The SXFM analysis (2D elemental maps) of sectioned otoliths showed interesting results (Fig. 6), complementary to the ones obtained with the LA-ICPMS transects (Fig. 3). For example, 2D elemental maps for Sr:Ca in the shortspine thornyhead (SST), longspine thornyhead (LST), and the Dover sole showed an increasing trend from core to edge (Fig. 6), being potentially related to the fishes' ontogenetic migration from surface waters (low salinity/warmer) to deeper waters (higher salinity/colder). Interestingly, we also observed Fe:Ca in the otolith of a bearded goby territorial male, suggesting that it has incorporated the reduced iron (Fe⁺²) after its larval stage. Together with Fe:Ca, a structurally similar Zn:Ca outer core ring suggests that this goby had spent a few weeks under very low oxygen waters. Iron and zinc elemental ratios show promise for tracking low oxygen exposures of OMZ-dwelling fishes as their concentrations increase from around 500 to 2000 m in the Pacific Ocean (Johnson K.S., 2021) and iron is high between 200 and 500 m in the Benguela Current Ecosystem in the Eastern South Atlantic Ocean (Liu et al., 2022), but increased instrumental resolution in otolith mapping (i.e., dwell-time/pixel) and water elemental analysis are needed to extensively test these relationships.

4.4. Which elements could be a proxy for fish exposure to low pH waters in OMZs-CMZs?

OMZs are also Carbon Maximum Zones (CMZ) and have naturally low pH waters because microbial respiration produces carbon dioxide (CO₂) and carbonic acid (H_2CO_3) while consuming oxygen, causing pH and oxygen levels to covary in these systems (Brewer and Peltzer, 2009; Paulmier et al., 2011). In the search for differences in elemental composition at different pH levels, Moreau et al. (1983) observed that manganese, zinc and strontium were 1.6, 1.3 and 1.2 higher in the opercula and scales of brook trout *Salvelinus fontinalis* in acidified lakes (pH 5.2–5.5) than in nonacidified lakes (pH 6.8–7.0). We observed higher ratios of manganese and strontium for the OMZ fishes (Figs. 3–5), which coincides with Moreau et al. (1983) observations. In our study, this indicates that the giant sea bass were encountering consistently higher pH waters (pH = 8.1) than the deep-sea fish caught in the OMZs (pH = 7.5) (Alin et al., 2012). Controlled experiments investigating the effect of pH and pCO_2 on otolith chemistry are scarce, limited to a

diadromous species (Martino et al., 2017), early life stages (Munday et al., 2011; Hurst et al., 2012) and with the measurement of the trace elements ¹¹B, ²³⁸U, ⁶⁵Cu, ²³Na, ⁷Li, ²⁵Mg, ⁴³Ca, ⁵⁵Mn, ⁸⁸Sr and ¹³⁸Ba. Overall, these studies did not detect significant variation in elemental concentrations between ambient and elevated *p*CO₂ treatments. Our analysis suggests that strontium, manganese, and zinc may work as indicators of fish exposure to low-pH and low-O₂ typical of OMZs-CMZs, but future experimental work is necessary to test the elemental-pH dependency. This is relevant as there is an ongoing and rapid pH decrease over the past 30 years in the SCB, at rates of 0.001–0.0015 yr⁻¹ at 500 m depth (Meinvielle and Johnson, 2013).

4.5. Could marine heat waves alter the chemistry of otoliths?

The differences observed at the edge of fish otoliths collected before and after "the Blob" are intriguing, especially for the redox sensitive element bromine (Fig. 6). "The Blob" was a superficial phenomenon that affected water temperatures down to ~ 100 m deep (Bond, et al., 2015). Therefore, its potential effects on OMZ fishes would be through direct pathways, such as reducing vertical transport of trace metals to the depths, potentially affecting the bioavailability of trace metals (e.g., scavenging) and indirect pathways that affect oxygen levels and/or food availability at depth. For example, during the Blob, primary productivity at the surface was reduced (Gómez-Ocampo et al., 2018), which would decrease microbial remineralization process and thus increase O₂ levels inside the upper OMZs, similar to what occurs during El Niño years (Mogollón and Calil 2017). Indeed, oxygen levels were higher in 2015, at least down to ~ 100 m deep (Brodeur et al., 2019). Reductions in phytoplankton biomass in surface waters likely also reduced food inputs to deeper habitats, potentially affecting the metabolism of higher trophic levels, including thornyheads. How the interaction of elevated oxygen levels and reduced food sources interactively affected the chemistry of deep-sea fish otoliths remains unclear and could be the focus of future research.

4.6. Thermal history reconstruction based on δ ¹⁸O

Using otolith $\delta^{18}O$ ratios, we reconstructed the thermal history of six deep-sea fishes and the giant sea bass. Although our sample sizes are small and results should be interpreted with caution, this study offers a first assessment of their ontogenetic movements and thermal histories, which had never been estimated before. This is mainly because of the impracticability of tagging deep-sea fish, which can suffer barotrauma, or because large species are often hard to find due to their low population sizes, such as occurs for the giant sea bass. In addition, tagging methods cannot track individuals for long periods of time (e.g., many decades) while otolith $\delta^{18}O$ can provide this finer temporal resolution.

The thermal histories of our species were considerably different, especially for the bearded gobies from Namibia and the demersal fish from SCB, suggesting that indeed low oxygen and pH waters typical of OMZs-CMZs (blue rectangles on Fig. 7) led to the resemblance of their otolith elemental composition (Fig. 2A).

Although shortspine and longspine thornyheads support a commercially important fishery, there is limited information about their ecology, growth rates, movement patterns, life histories and capacity to withstand fishing pressure (Jacobson and Vetter, 1996; Pearson and Gunderson, 2003; Echave, 2017). Longspine thornyheads are oviparous and produce gelatinous egg sacs that float to the surface waters where hatching and larval development occurs at warmer water temperatures. Juveniles of longspines remain in surface waters for approximately 20 months, prior to their settlement at depths between 600 and 1200 m deep (Moser, 1974; Wakefield, 1990); as adults, they are OMZ specialists, found only in deep waters (600–1400 m) (Jacobson and Vetter, 1996). Accordingly, the thermal history reconstruction for the longspine thornyhead showed a clear ontogenetic vertical migration into the cold waters of the Southern California Bight OMZ (Fig. 7A).

The shortspine thornyhead, conversely, is believed to settle at approximately 100 m depth on the shelf and perform a relatively steady ontogenetic migration into deeper waters (Moser, 1974; Jacobson and Vetter, 1996). However, previous research has debated its main centers of abundance at shallower waters at 180–440 m (Moser, 1974) or at deeper waters at 600–1000 m (Jacobson and Vetter, 1996). The estimated habitat temperature herein reconciles both views, as this species can remain for longer periods of time either at shallower or deeper depths, and its thermal history reconstruction was variable, suggesting at least three major migrations into different water depths for this individual (Fig. 7C).

The estimated habitat temperature for the Dover sole (Fig. 7B) agreed with the known life-history strategy for this species; they are born in shallow waters of the continental shelf and, as they grow, they gradually move down the continental slope into deeper waters to reproduce (Jacobson and Hunter, 1993).

The short-lived specimens observed were the black brotulas from the Gulf of California (<1 years), the bearded gobies (~2 to 7 years) from the Namibian shelf and the rubynose brotulas (~ 10 years) from Southern California Bight. Information on population dynamics is scarce for the black brotulas and rubynose brotulas (Gibbs, 1991; Morales-Azpeitia et al., 2018; Gallo et al., 2019), despite their incredible abilities to withstand hypoxic and conditions closer to anoxia. The rubynose brotula is believed to spend its larval and juvenile stages in the deep scattering layer (300-500 m deep) before moving to the benthos (>800 m) as adults (Gibbs, 1991, 1999). This assumption does not match our temperature data (Fig. 7D), which indicated that this species undergoes an ontogenetic migration from surface into deeper waters. The two black brotulas presented similar ranges of habitat temperature from around 4 °C to 16.5 °C (Fig. 7E and F). These temperature ranges match recent data that reflect the occurrence of eggs and larvae in surface waters and juveniles and adults up to ~ 1000 m depth (Zamorano et al., 2014). This species likely plays a crucial ecological role, since its larvae have been reported as among the most abundant during an extensive exploration of the continental slope off the Mexican Pacific margin (Zamorano et al., 2014). Recently, both the black brotula and rubynose brotula were observed at 1,097 and 2,000 m around Vancouver Island, in British Columbia, Canada (Hanke et al., 2015), revealing how little we still know about the basic biology of these species, as their depth ranges are still unknown. Future studies should expand the analysis of Mn and $\delta^{18}O$ in black brotula otoliths to understand how the interaction of low oxygen and temperature conditions affect the ecology of the species.

Bearded gobies reproduce on the seabed in nests, usually during spring and summer in the southern hemisphere. Territorial males are assumed to remain at the bottom for parental care of the eggs longer than females and sneaker males. Experiments have demonstrated that territorial males cared for egg clutches for at least six days at 17 °C (Skrypzeck et al., 2014), whereas assumed sneakers that have similar morphology of females (Salvanes et al., 2018) would be "free" to undertake diel vertical migrations and thus visit better oxygenated upper waters. After hatching, larvae and juvenile are pelagic and abundant in the upper 50 m layer, experiencing between 16 and 22.5 $^{\circ}\text{C}$ in the north of Namibia (O'Toole, 1978). As the juveniles grow and mature, they move further offshore to the seabed to reproduce, usually under very low oxygen conditions (Salvanes et al., 2015; Salvanes and Gibbons, 2018). This life-history strategy agrees with the thermal history reconstructed based on otolith $\delta^{18}O$ values (Fig. 7G and H). Intriguingly, we also observed a much higher temperature exposure for the sneaker male (#3081) (Fig. 7G). This individual was born during the strong Benguela Niño in 2010/2011. This event began in November 2010, lasted five months, and peaked in January 2011, resulting in monthly water temperatures anomalies up to 4 °C above the average (Rouault et al., 2018). This El Niño imparted the lowest otolith δ^{18} O values and highest reconstructed temperatures of up to \sim 25 $^{\circ}C$ on this male's otolith (#3081). The female goby (#3044) was mature at the time of collection

(3 years old) and her otolith did not indicate such an anomalous warm pattern, suggesting that it may remain closer to the substrate, perhaps to reproduce under low temperatures and oxygen conditions. This is also supported by the highest Mn:Ca ratios observed for two female gobies (Fig. 3A).

The giant sea bass were the oldest individuals analyzed, thus allowing the reconstruction of habitat temperature back to the early 1970s (Fig. 7I and J). Specimen #170506 showed a maximum temperature ($\sim 27^{\circ}$ C) in the year 1983, while the specimen #170606 exhibited maximum temperatures in the years 1999 and 2011. These patterns were potentially associated to the very strong El Niño events of 1983 and 1997/98. These individuals were caught off the coast of Guerrero Negro, in Baja California Sur (Mexico), where local fishermen have observed individuals in shallower bays, which can explain the relatively warm temperatures for some years in the otolith record. Overall, the thermal history of the giant sea bass appears to be more variable than the deepsea OMZ fishes, suggesting that these sea giants might endure long latitudinal migratory movements between USA and Mexico waters (Baldwin and Keiser, 2008; Gaffney et al., 2007), and/or experience variable water oxygen isotopic composition and ambient temperature linked to upwelling pulses (Sautter and Thunell, 1991; Low et al., 2021).

Reconstructing the thermal histories of these fishes can provide a baseline for future comparisons of fish exposed to warmer ocean conditions due to climate change. Because the deep-sea fish analyzed here are believed to be less mobile after they settle in the OMZ, their adult stages may accurately reflect the environmental temperatures, pH, and low oxygen conditions characteristic of the deep sea.

5. Conclusion

This research extends previous otolith studies of elemental proxies in hypoxic estuaries and enclosed seas to open ocean and deep-sea settings. Deep-sea fishes from different ocean basins (i.e., the Northeast Pacific and the Southeast Atlantic) and with different life-history traits (such as longevity and thermal histories estimated by δ^{18} O) exhibited similar elemental composition in their otoliths driven largely by Sr:Ca, Mn:Ca, Ba:Ca, Cu:Ca and Mg:Ca ratios. These deep-sea fishes have in common the extremely low oxygen conditions they have experienced for most of their lives beneath waters marked by high levels of primary productivity. We hypothesize that the Oxygen Minimum Zones and Carbon Maximum Zones associated with the EBUS have a unique biogeochemistry that can affect otolith chemistry in similar ways. Our results suggest manganese, strontium, and zinc as potential tracers for oxygen and pH in deep-sea fishes, with higher Me:Ca ratios in otoliths associated with lower oxygen and pH waters in OMZ-CMZs. Individual thermal histories based on δ^{18} O are shown to offer insight into deep-sea fish exposures to low oxygen and pH. New proxies for hypoxic and acidic water conditions are particularly needed in economically important EBUS such as the Southern California Bight, where dissolved oxygen and pH have been decreasing for the past 30 years, and the Namibian shelf, where warming trends and intensification of upwelling winds can expand the already massive hypoxic and sulphidic waters of the continental shelf. We encourage further work to examine applicability of our findings in other deep-sea basins and hypoxic settings.

Declaration of competing interest

The authors declare that they have no known competing financial interests or personal relationships that could have appeared to influence the work reported in this paper.

Data availability

Data will be made available on request.

Acknowledgements

We thank the Instructional Support Specialist Debra Driscoll at the State University of New York College of Environmental Science and Foresry (SUNY-ESF) for support during the LA-ICPMS analyses, and Louisa Smieska at the Cornell High Energy Synchrotron Source (CHESS) for support during the SXFM analyses.

This work is based upon research conducted at the CHESS which is supported by the National Science Foundation (NSF) under award DMR-1332208.

Analyses at the W.M. Keck Center for Isotope Geochemistry at the University of California Los Angeles (UCLA) were supported by a grant from the NSF Instrumentation and Facilities Program. Southern California fishes were collected on research cruises supported by UC Ship Funds, the CCE LTER Program, the NOAA Groundfish Trawl Survey, and MBARI. We thank the crew on the RV Blue Sea and RV Dr. Fridtjof Nansen, Frank Midtøy and Bronwen Currie for help to collect the bearded goby samples, and the University of Bergen and the National Research Foundations of Norway and South Africa (Grant number 180329/S50) for funding. Giant sea bass samples were obtained under research supported by Mia J. Tegner Research Fellowship at Scripps Institution of Oceanography and PADI Foundation (2017: 29020; 2018; 33095) to A.R. Valdez A.R. Valdez thanks the support of UC Mexus-CONACYT doctoral fellowship 160083, and Shirley Boyd Memorial Endowment at SIO - University of California San Diego (UCSD). L.A. Levin was supported by NSF OCE1829623 and NOAA CHRP award NA18NOS4780172. N.D. Gallo was funded by a QUEST grant to Brice X. Semmens. L.M. Cavole was supported by CNPq grant 213540/2014-2. K. E. Limburg was supported by NSF OCE 1923965.

Appendix A. Supplementary data

Supplementary data to this article can be found online at https://doi.org/10.1016/j.dsr.2022.103941.

References

- Abshire, M.L., Romaniello, S.J., Kuzminov, A.M., Cofrancesco, J., Severmann, S., Riedinger, N., 2020. Uranium isotopes as a proxy for primary depositional redox conditions in organic-rich marine systems. Earth Planet Sci. Lett. 529, 115878.
- Alin, S.R., Feely, R.A., Dickson, A.G., Hernández-Ayón, J.M., Juranek, L.W., Ohman, M. D., Goericke, R., 2012. Robust empirical relationships for estimating the carbonate system in the southern California Current System and application to CalCOFI hydrographic cruise data (2005–2011). J. Geophys. Res.: Oceans 117 (C5).
- Allen, L.G., Andrews, A.H., 2012. Bomb radiocarbon dating and estimated longevity of Giant Sea Bass (Stereolepis gigas). Bull. South Calif. Acad. Sci. 111 (1), 1–14.
- Altenritter, M.E., Cohuo, A., Walther, B.D., 2018. Proportions of demersal fish exposed to sublethal hypoxia revealed by otolith chemistry. Mar. Ecol. Prog. Ser. 589, 193–208.
- Baldwin, D.S., Keiser, A., 2008. Giant Sea Bass, Stereolepis Gigas. Status of the Fisheries. Report California Department of Fish and Game, p. 8. https://nrm.dfg.ca.gov/FileHandler.ashx?DocumentID=34433&inline=true.
- Bennett, W.W., Canfield, D.E., 2020. Redox-sensitive trace metals as paleoredox proxies: a review and analysis of data from modern sediments. Earth Sci. Rev. 204, 103175. Bograd, S.J., Castro, C.G., Di Lorenzo, E., Palacios, D.M., Bailey, H., Gilly, W., Chavez, F. P., 2008. Oxygen declines and the shoaling of the hypoxic boundary in the California Current. Geophys. Res. Lett. 35 (12).
- Bograd, S.J., Buil, M.P., Di Lorenzo, E., Castro, C.G., Schroeder, I.D., Goericke, R., Anderson, C.R., Benitez-Nelson, C., Whitney, F.A., 2015. Changes in source waters to the southern California Bight. Deep Sea Res. Part II Top. Stud. Oceanogr. 112, 42–52.
- Bond, N.A., Cronin, M.F., Freeland, H., Mantua, N., 2015. Causes and impacts of the 2014 warm anomaly in the NE Pacific. Geophys. Res. Lett. 42 (9), 3414–3420.
- Breitburg, D., Levin, L.A., Oschlies, A., Grégoire, M., Chavez, F.P., Conley, D.J., Garçon, V., Gilbert, D., Gutiérrez, D., Isensee, K., Jacinto, G.S., 2018. Declining oxygen in the global ocean and coastal waters. Science 359 (6371), eaam7240.
- Brewer, P.G., Peltzer, E.T., 2009. Limits to marine life. Science 324 (5925), 347–348.
 Brodeur, R.D., Auth, T.D., Phillips, A.J., 2019. Major shifts in pelagic micronekton and macrozooplankton community structure in an upwelling ecosystem related to an unprecedented marine heatwave. Front. Mar. Sci. 6, 212.
- Bruland, K.W., Lohan, M.C., 2004. Controls of trace metals in sea water. In: Holland, H. D., Turekian, K.K. (Eds.), Treatise on Geochemistry 6, 23–47.
- Butler, J.L., Kastelle, C., Rubin, K., Kline, D., Heijins, H., Jacobson, L., Andrews, A., Wakefield, W.W., 1995. Age Determination of Shortspine Thornyhead, Sebastolobus Alascanus, Using Otolith Sections and 210Pb: 226Ra Ratio. Admin. Rep. No. LJ-95-12. National Marine Fisheries Service, Southwest Fisheries Science Center, La Jolla, Calif.

- Calvert, S.E., Price, N.B., 1983. Geochemistry of Namibian shelf sediments. In: Coastal Upwelling its Sediment Record. Springer, Boston, MA, pp. 337–375.
- Campana, S.E., Jones, C.M., 1992. Analysis of otolith microstructure data. In: Stevenson, D.K., Campana, S.E. (Eds.), Otolith Microstructure Examination and Analysis. Canadian Special Publication of Fisheries Aquatic Sciences 117, 73–100. Department of Supply and Services, Ottawa.
- Carr, M.E., 2002. Estimation of potential productivity in Eastern Boundary Currents using remote sensing. Deep Sea Res. Part II Top. Stud. Oceanogr. 49 (1–3), 59–80.
- Cavole, L.M., Demko, A.M., Diner, R.E., Giddings, A., Koester, I., Pagniello, C.M., Paulsen, M.L., Ramirez-Valdez, A., Schwenck, S.M., Yen, N.K., Zill, M.E., 2016. Biological impacts of the 2013–2015 warm-water anomaly in the Northeast Pacific: winners, losers, and the future. Oceanography 29 (2), 273–285.
- Chavez, F.P., Messié, M., 2009. A comparison of eastern boundary upwelling ecosystems. Prog. Oceanogr. 83 (1–4), 80–96.
- Clements, S.C., Takeshita, Y., Dickson, A., Martz, T., Smith, J.E., 2020. Scripps Ocean Acidification Real-Time (SOAR) Dataset. Scripps Institution of Oceanography, La Jolla, CA. https://coralreefecology.sioword.ucsd.edu/wp-content/uploads/sites/431/2020/05/SOAR_SP2020_Report_draftFinal-2.jpg.
- Currie, B., Utne-Palm, A.C., Salvanes, A.G.V., 2018. Winning ways with hydrogen sulphide on the Namibian shelf. Front. Mar. Sci. 5, 341.
- Dailey, M.D., Reish, D.J., Anderson, J.W. (Eds.), 1993. Ecology of the Southern California Bight: a Synthesis and Interpretation. Univ of California Press.
- Devereux, I., 1967. Temperature measurements from oxygen isotope ratios of fish otoliths. Science 155 (3770), 1684–1685.
- Dorval, E., Methot, R.D., Taylor, I.G., Piner, K.R., 2022. Otolith chemistry indicates age and region of settlement of immature shortspine thornyhead *Sebastolobus alascanus* in the eastern Pacific Ocean. Mar. Ecol. Prog. Ser. 693, 157–175.
- Echave, K.B., 2017. First results of the tagging of shortspine thornyhead, *Sebastolobus alascanus*. In: Alaska, vol. 195. Fisheries Research, pp. 46–51.
- Elsdon, T.S., Gillanders, B.M., 2002. Interactive effects of temperature and salinity on otolith chemistry: challenges for determining environmental histories of fish. Can. J. Fish. Aquat. Sci. 59 (11), 1796–1808.
- Esbaugh, A.J., Heuer, R., Grosell, M., 2012. Impacts of ocean acidification on respiratory gas exchange and acid-base balance in a marine teleost, Opsanus beta. J. Comp. Physiol. B 182 (7), 921–934.
- Figueiredo, C., Baptista, M., Grilo, T.F., Caetano, M., Markaida, U., Raimundo, J., Rosa, R., 2020. Bioaccumulation of trace elements in myctophids in the oxygen minimum zone ecosystem of the Gulf of California. In: Oceans, vol. 1. MDPI, p. 4. No.
- Fitch, J.E., Lavenberg, R.J., Fitch, S., 1971. Marine Food and Game Fishes of California, vol. 28. Univ of California Press.
- Gaffney, P.M., Rupnow, J., Domeier, M.L., 2007. Genetic similarity of disjunct populations of the giant sea bass Stereolepis gigas. J. Fish. Biol. 70, 111–124.
- Gallo, N.D., Levin, L.A., 2016. Fish ecology and evolution in the world's oxygen minimum zones and implications of ocean deoxygenation. Adv. Mar. Biol. 74, 117–198.
- Gallo, N.D., 2018. Influence of Ocean Deoxygenation on Demersal Fish Communities: Lessons from Upwelling Margins and Oxygen Minimum Zones. PhD. Dissertation, University of California, San Diego, 2018.
- Gallo, N.D., Levin, L.A., Beckwith, M., Barry, J.P., 2019. Home sweet suboxic home: remarkable hypoxia tolerance in two demersal fish species in the Gulf of California. Ecology 100 (3), e02539.
- Gallo, N.D., Beckwith, M., Wei, C.L., Levin, L.A., Kuhnz, L., Barry, J.P., 2020. Dissolved oxygen and temperature best predict deep-sea fish community structure in the Gulf of California with climate change implications. Mar. Ecol. Prog. Ser. 637, 159–180.
- Gerringer, M.E., Andrews, A.H., Huss, G.R., Nagashima, K., Popp, B.N., Linley, T.D., Gallo, N.D., Clark, M.R., Jamieson, A.J., Drazen, J.C., 2018. Life history of abyssal and hadal fishes from otolith growth zones and oxygen isotopic compositions. Deep Sea Res. Oceanogr. Res. Pap. 132, 37–50.
- Gibbs, M.A., 1991. Notes on the distribution and morphology of the rubynose brotula (Cataetyx rubrirostris) off central California. Calif. Fish Game 77, 149–152.
- Gibbs, M.A., 1999. Lateral line morphology and cranial osteology of the rubynose brotula, Cataetyx rubrirostris. J. Morphol. 241 (3), 265–274.
- Gilly, W.F., Beman, J.M., Litvin, S.Y., Robison, B.H., 2013. Oceanographic and biological effects of shoaling of the oxygen minimum zone. Ann. Rev. Mar. Sci 5, 393–420.
- Gómez-Ocampo, E., Gaxiola-Castro, G., Durazo, R., Beier, E., 2018. Effects of the 2013-2016 warm anomalies on the California Current phytoplankton. Deep Sea Res. Part II Top. Stud. Oceanogr. 151, 64–76.
- Gower, J.C., 1966. Some distance properties of latent root and vector methods used in multivariate analysis. Biometrika 53 (3–4), 325–338.
- Grossman, E.L., 1984. Stable isotope fractionation in live benthic foraminifera from the Southern California Borderland. Palaeogeogr. Palaeoclimatol. Palaeoecol. 47 (3–4), 301–327.
- Grupe, B.M., Krach, M.L., Pasulka, A.L., Maloney, J.M., Levin, L.A., Frieder, C.A., 2015. Methane seep ecosystem functions and services from a recently discovered southern California seep. Mar. Ecol. 36, 91–108.
- Hanke, G., Gillespie, G., Fong, K., Boutillier, J., Nielsen, J., Møller, P., Bedard, J., Riley, J., 2015. New records of seven cusk-eels (Ophidiidae) and brotulas (Bythitidae) in coastal waters of British Columbia, Canada. Northwest. Nat. 96 (1), 71–80.
- Hawk, H.A., Allen, L.G., 2014. Age and Growth of the Giant Sea Bass, Stereolepis Gigas, vol. 55. CalCOFI Report, pp. 128–134.
- Helly, J.J., Levin, L.A., 2004. Global distribution of naturally occurring marine hypoxia on continental margins. Deep Sea Res. Oceanogr. Res. Pap. 51 (9), 1159–1168.
- Hendrickx, M., Serrano, D., 2014. Effects of the oxygen minimum zone on squat lobster distributions in the Gulf of California, Mexico. Open Life Sci. 9 (1), 92–103.

- Høie, H., Otterlei, E., Folkvord, A., 2004. Temperature-dependent fractionation of stable oxygen isotopes in otoliths of juvenile cod (*Gadus morhua*). ICES (Int. Counc. Explor. Sea) J. Mar. Sci. 61, 243–251.
- Hopkinson, B.M., Barbeau, K.A., 2007. Organic and redox speciation of iron in the eastern tropical North Pacific suboxic zone. Mar. Chem. 106 (1–2), 2–17.
- Hunter, J.R., Butler, J.L., Kimbrell, C.A.R.O.L., Lynn, E.A., 1990. Bathymetric patterns in size, age, sexual maturity, water content, and caloric density of Dover sole, *Microstomus pacificus*. CalCOFI Invest. Rep 31, 132–144.
- Hurst, T.P., Fernandez, E.R., Mathis, J.T., Miller, J.A., Stinson, C.M., Ahgeak, E.F., 2012. Resiliency of juvenile walleye pollock to projected levels of ocean acidification. Aquat. Biol. 17 (3), 247–259.
- Hüssy, K., Limburg, K.E., de Pontual, H., Thomas, O.R., Cook, P.K., Heimbrand, Y., Blass, M., Sturrock, A.M., 2020. Trace element patterns in otoliths: the role of biomineralization. Reviews in Fisheries Science & Aquaculture 1–33.
- Hutchings, L., Van der Lingen, C.D., Shannon, L.J., Crawford, R.J.M., Verheye, H.M.S., Bartholomae, C.H., Van der Plas, A.K., Louw, D., Kreiner, A., Ostrowski, M., Fidel, Q., 2009. The Benguela Current: an ecosystem of four components. Prog. Oceanogr. 83 (1–4), 15–32.
- Jacobson, L.D., Hunter, J.R., 1993. Bathymetric demography and management of Dover sole. N. Am. J. Fish. Manag. 13 (3), 405–420.
- Jacobson, L.D., Vetter, R.D., 1996. Bathymetric demography and niche separation of thornyhead rockfish: Sebastolobus alascanus and Sebastolobus altivelis. Can. J. Fish. Aquat. Sci. 53 (3), 600–609.
- Jochum, K.P., Weis, U., Stoll, B., Kuzmin, D., Yang, Q., Raczek, I., Jacob, D.E., Stracke, A., Birbaum, K., Frick, D.A., Günther, D., 2011. Determination of reference values for NIST SRM 610–617 glasses following ISO guidelines. Geostand. Geoanal. Res. 35 (4), 397–429.
- Johnson, K.S., Berelson, W.M., Coale, K.H., Coley, T.L., Elrod, V.A., Fairey, W.R., Iams, H.D., Kilgore, T.E., Nowicki, J.L., 1992. Manganese flux from continental margin sediments in a transect through the oxygen minimum. Science 257 (5074), 1242–1245.
- Johnson, K.S., Coale, K.H., Berelson, W.M., Gordon, R.M., 1996. On the formation of the manganese maximum in the oxygen minimum. Geochem. Cosmochim. Acta 60 (8), 1291–1299.
- Johnson, K.S.. Periodic table of elements in the Ocean. https://www.mbari.org/science/upper-ocean-systems/chemical-sensor-group/periodic-table-of-elements-in-the-ocean/. (Accessed 20 April 2021).
- Kalish, J.M., 1989. Otolith microchemistry: validation of the effects of physiology, age and environment on otolith composition. J. Exp. Mar. Biol. Ecol. 132 (3), 151–178.
- Kassambara, A., 2020. Ggpubr: 'ggplot2' Based Publication Ready Plots. R package version 0.2.5. https://CRAN.R-project.org/package=ggpubr.
 Kastelle, C.R., Kimura, D.K., Jay, S.R., 2000. Using 210Pb/226Ra disequilibrium to
- Kastelle, C.R., Kimura, D.K., Jay, S.R., 2000. Using 210Pb/226Ra disequilibrium to validate conventional ages in Scorpaenids (genera Sebastes and Sebastolobus). Fish. Res. 46 (1–3), 299–312.
- Keeling, R.F., Garcia, H.E., 2002. The change in oceanic O₂ inventory associated with recent global warming. Proc. Natl. Acad. Sci. USA 99 (12), 7848–7853.
- Keeling, R.F., Körtzinger, A., Gruber, N., 2010. Ocean deoxygenation in a warming world. Ann. Rev. Mar. Sci 2, 199–229.
- Kline, D.E., 1996. Radiochemical Age Verification for Two Deep-Sea Rockfishes: Sebastolobus Altivelis and S. Alascanus. M.S. Thesis. Moss Landing Marine Laboratories, San Jose State University, CA, p. 124.
- Koslow, J.A., Goericke, R., Lara-Lopez, A., Watson, W., 2011. Impact of declining intermediate-water oxygen on deepwater fishes in the California Current. Mar. Ecol. Prog. Ser. 436, 207–218.
- Kwan, G.T., Tresguerres, M., 2022. Elucidating the acid-base mechanisms underlying otolith overgrowth in fish exposed to ocean acidification. Sci. Total Environ. 823, 153690.
- Levin, L.A., 2003. Oxygen minimum zone benthos: adaptation and community response to hypoxia. In: Oceanography and Marine Biology, vol. 41. Taylor & Francis, London, pp. 1–45.
- Levin, L.A., Ekau, W., Gooday, A.J., Jorissen, F., Middelburg, J.J., Naqvi, S.W.A., Neira, C., Rabalais, N.N., Zhang, J., 2009. Effects of Natural and Human-Induced Hypoxia on Coastal Benthos.
- Levin, I.A., Hönisch, B., Frieder, C.A., 2015. Geochemical proxies for estimating faunal exposure to ocean acidification. Oceanography 28 (2), 62–73.
- Levin, L.A., Girguis, P.R., German, C.R., Brennan, M.L., Tüzün, S., Wagner, J., Smart, C., Kruger, A., Inderbitzen, K., Le, J., Martinez, M., 2016. Exploration and discovery of methane seeps and associated communities in the California Borderland. In: Bell, K. L.C., Brennan, M.L., Flanders, J., Raineault, N.A., Wagner, K. (Eds.), New Frontiers in Ocean Exploration: the E/V Nautilus and NOAA Ship Okeanos Explorer 2015 Field Season. The Oceanography Society, Rockville, MD, pp. 40–43. https://doi.org/10.5670/oceanog.2016.supplement.01.
- Liu, T., Krisch, S., Xie, R.C., Hopwood, M.J., Dengler, M., Achterberg, E.P., 2022. Sediment release in the Benguela Upwelling System dominates trace metal input to the shelf and eastern South Atlantic Ocean. Global Biogeochem. Cycles 36 (9). https://doi.org/10.1029/2022GB007466 e2022GB007466.
- Love, M.S., Yoklavich, M., Thorsteinson, L.K., 2002. The Rockfishes of the Northeast Pacific. Univ of California Press.
- Low, N.H., Micheli, F., Aguilar, J.D., Arce, D.R., Boch, C.A., Bonilla, J.C., Bracamontes, M.Á., De Leo, G., Diaz, E., Enríquez, E., Hernandez, A., 2021. Variable coastal hypoxia exposure and drivers across the southern California Current. Sci. Rep. 11 (1), 1–10.
- Limburg, K.E., Olson, C., Walther, Y., Dale, D., Slomp, C.P., Høie, H., 2011. Tracking Baltic hypoxia and cod migration over millennia with natural tags. Proc. Natl. Acad. Sci. USA 108 (22), E177–E182.

- Limburg, K.E., Walther, B.D., Lu, Z., Jackman, G., Mohan, J., Walther, Y., Nissling, A., Weber, P.K., Schmitt, A.K., 2015. In search of the dead zone: use of otoliths for tracking fish exposure to hypoxia. J. Mar. Syst. 141, 167–178.
- Limburg, K.E., Casini, M., 2018. Effect of marine hypoxia on Baltic sea cod Gadus morhua: evidence from otolith chemical proxies. Front. Mar. Sci. 5, 482.
- Mackas, D.L., Strub, P.T., Thomas, A., Montecino, V., 2006. Eastern regional ocean boundaries pan-regional overview. In: Robinson, A.R., Brink, K. (Eds.), The Sea, vol. 14a. Harvard University Press, Cambridge, Massachussetts, pp. 21–60.
- Martino, J., Doubleday, Z.A., Woodcock, S.H., Gillanders, B.M., 2017. Elevated carbon dioxide and temperature affects otolith development, but not chemistry, in a diadromous fish. J. Exp. Mar. Biol. Ecol. 495, 57–64.
- McClatchie, S., Goericke, R., Cosgrove, R., Auad, G., Vetter, R., 2010. Oxygen in the Southern California Bight: multidecadal trends and implications for demersal fisheries. Geophys. Res. Lett. 37 (19).
- Meinvielle, M., Johnson, G.C., 2013. Decadal water-property trends in the California Undercurrent, with implications for ocean acidification. J. Geophys. Res.: Oceans 118 (12), 6687–6703.
- Melo, Y.C., Le Clus, F., 2005. Growth and reproduction of the pelagic goby *Sufflogobius bibarbatus* off the Orange River, southern Africa. Afr. J. Mar. Sci. 27 (1), 265–273.
- Mogollón, R., Calil, P.H., 2017. On the effects of ENSO on ocean biogeochemistry in the Northern Humboldt Current System (NHCS): a modeling study. J. Mar. Syst. 172, 137–159.
- Morales-Azpeitia, R., López-Martínez, J., Herrera-Valdivia, E., Acevedo-Cervantes, A., 2018. Population dynamics of black brotula (Cherublemma emmelas) in deep waters of the Gulf of California. Latin american journal of aquatic research 46 (5), 1103–1109
- Moreau, G., Barbeau, C., Frenette, J.J., Saint-Onge, J., Simoneau, M., 1983. Zinc, manganese, and strontium in opercula and scales of brook trout (Salvelinus fontinalis) as indicators of lake acidification. Can. J. Fish. Aquat. Sci. 40 (10), 1685–1691.
- Morford, J.L., Emerson, S., 1999. The geochemistry of redox sensitive trace metals in sediments. Geochem. Cosmochim. Acta 63 (11–12), 1735–1750.
- Moser, H.G., 1974. Development and distribution of larvae and juveniles of Sebastolobus (Pisces: family Scorpaenidae). Fish. Bull. 72 (4), 865–884.
- Munday, P.L., Hernaman, V., Dixson, D.L., Thorrold, S.R., 2011. Effect of ocean acidification on otolith development in larvae of a tropical marine fish. Biogeosciences 8, 1631–1641.
- Nielsen, J.G., Cohen, D.M., Markle, D.F., Robins, C.R., 1999. Ophidiiform fishes of the world (Order Ophidiiformes). An annotated and illustrated catalogue of pearlfishes, cusk-eels, brotulas and other ophidiiform fishes known to date. Fao Fish. Synop. 125 (18). 178 (Rome: FAO).
- O'Toole, M.J., 1978. Development, distribution and relative abundance of the larvae and early juveniles of the pelagic goby *Sufflogobius bibarbatus* (von Bonde) off South West Africa 1972–1974. Sea Fish. Branch Invest. Rep. 116, 1–28.
- Paulmier, A., Ruiz-Pino, D., 2009. Oxygen minimum zones (OMZs) in the modern ocean. Prog. Oceanogr. 80 (3–4), 113–128.
- Paulmier, A., Ruiz-Pino, D., Garçon, V., 2011. CO₂ maximum in the oxygen minimum zone (OMZ). Biogeosciences 8 (2), 239–252.
- Pearcy, W.G., Hancock, D., 1978. Feeding Habits of Dover Sole, Microstomus pacificus; Rex Sole, Glyptocephalus zachirus; Slender Sole, Lyopsetta exilis; and Pacific Sanddab, Citharichthys Sordidus, in a Region of Diverse Sediments and Bathymetry off Oregon.
- Pearson, K.E., Gunderson, D.R., 2003. Reproductive biology and ecology of shortspine thornyhead rockfish, Sebastolobus alascanus, and longspine thornyhead rockfish, S. altivelis, from the northeastern Pacific Ocean. Environ. Biol. Fish. 67 (2), 117–136.
- Pitcher, G.C., Aguirre-Velarde, A., Breitburg, D., Cardich, J., Carstensen, J., Conley, D.J., Dewitte, B., Engel, A., Espinoza-Morriberón, D., Flores, G., Garçon, V., 2021. System controls of coastal and open ocean oxygen depletion. Prog. Oceanogr. 197, 102613.
- Pörtner, H., 2001. Climate change and temperature-dependent biogeography: oxygen limitation of thermal tolerance in animals. Naturwissenschaften 88 (4), 137–146.
- Pörtner, H.O., 2021. Climate impacts on organisms, ecosystems and human societies: integrating OCLTT into a wider context. J. Exp. Biol. 224 (Suppl. 1).
- Ramfrez-Valdez, A., Rowell, T.J., Dale, K.E., Craig, M.T., Allen, L.G., Villaseñor-Derbez, J.C., Cisneros-Montemayor, A.M., Hernández-Velasco, A., Torre, J., Hofmeister, J., Erisman, B.E., 2021. Asymmetry across international borders: research, fishery and management trends, and economic value of the giant sea bass (Stereoleopis gigas). Fish Fish. 22 (6), 1392–1411.
- Rouault, M., Illig, S., Lübbecke, J., Koungue, R.A.I., 2018. Origin, development and demise of the 2010–2011 Benguela Niño. J. Mar. Syst. 188, 39–48.
- Salvanes, A.G., Utne-Palm, A.C., Currie, B., Braithwaite, V.A., 2011. Behavioural and physiological adaptations of the bearded goby, a key fish species of the extreme environment of the northern Benguela upwelling. Mar. Ecol. Prog. Ser. 425, 193–202
- Salvanes, A.G.V., Bartholomae, C., Yemane, D., Gibbons, M.J., Kainge, P., Krakstad, J.O., Rouault, M., Staby, A., Sundby, S., 2015. Spatial dynamics of the bearded goby and its key fish predators off Namibia vary with climate and oxygen availability. Fish. Oceanogr. 24, 88–101.
- Salvanes, A.G.V., Christiansen, H., Taha, Y., Henseler, C., Seivåg, M.L., Kjesbu, O.S., Folkvord, A., Utne-Palm, A.C., Currie, B., Ekau, W., van der Plas, A.K., 2018. Variation in growth, morphology and reproduction of the bearded goby (Sufflogobius bibarbatus) in varying oxygen environments of northern Benguela. J. Mar. Syst. 188, 81–97.
- Salvanes, A.G.V., Gibbons, M.J., 2018. Adaptation to hypoxic environments; bearded gobies Sufflogobius bibarbatus in the Benguela upwelling ecosystem. J. Fish. Biol. 92 (3), 752–772.

- Sautter, L.R., Thunell, R.C., 1991. Seasonal variability in the δ^{18} O and δ^{13} C of planktonic foraminifera from an upwelling environment: sediment trap results from the San Pedro Basin, Southern California Bight. Paleoceanography 6 (3), 307–334.
- Sarmiento, J.L., Hughes, T.M., Stouffer, R.J., Manabe, S., 1998. Simulated response of the ocean carbon cycle to anthropogenic climate warming. Nature 393 (6682), 245–249.
- Sato, K.N., Andersson, A.J., Day, J., Taylor, J.R., Frank, M.B., Jung, J.Y., McKittrick, J., Levin, L.A., 2018. Response of sea urchin fitness traits to environmental gradients across the Southern California oxygen minimum zone. Front. Mar. Sci. 5, 258.
- Schmidt, G.A., Bigg, G.R., Rohling, E.J., 1999. Global seawater oxygen-18 database v1.22. https://data.giss.nasa.gov/o18data/. (Accessed October 2022).
- Schmidtko, S., Stramma, L., Visbeck, M., 2017. Decline in global oceanic oxygen content during the past five decades. Nature 542 (7641), 335–339.
- Shiao, J.C., Sui, T.D., Chang, N.N., Chang, C.W., 2017. Remarkable vertical shift in residence depth links pelagic larval and demersal adult jellynose fish. Deep Sea Res. Oceanogr. Res. Pap. 121, 160–168.
- Skrypzeck, H., Salvanes, A.G.V., Currie, B., Kotze, A., 2014. First records of reproductive behaviour and early development of the bearded goby Sufflogobius bibarbatus. J. Fish. Biol. 84 (4), 1256–1261.
- Solé, V.A., Papillon, E., Cotte, M., Walter, P., Susini, J.A., 2007. A multiplatform code for the analysis of energy-dispersive X-ray fluorescence spectra. Spectrochim. Acta B Atom Spectrosc. 62 (1), 63–68.
- Staby, A., Krakstad, J.-O., 2006. Review of the state of knowledge, research (past and present) of the distribution, biology, ecology and abundance of non-exploited mesopelagic fish and the bearded goby (Sufflogobius bibarbatus) in the Benguela Ecosystem. In: Report on BCLME Project LMR/CF/03/08.
- Stramma, L., Schmidtko, S., Levin, L.A., Johnson, G.C., 2010. Ocean oxygen minima expansions and their biological impacts. Deep Sea Res. Oceanogr. Res. Pap. 57 (4), 587-595
- Stramma, L., Prince, E.D., Schmidtko, S., Luo, J., Hoolihan, J.P., Visbeck, M., Wallace, D. W., Brandt, P., Körtzinger, A., 2012. Expansion of oxygen minimum zones may reduce available habitat for tropical pelagic fishes. Nat. Clim. Change 2 (1), 33–37.
- Sturrock, A.M., Trueman, C.N., Milton, J.A., Waring, C.P., Cooper, M.J., Hunter, E., 2014. Physiological influences can outweigh environmental signals in otolith microchemistry research. Mar. Ecol. Prog. Ser. 500, 245–264.
- Sturrock, A.M., Hunter, E., Milton, J.A., Johnson, R.C., Waring, C.P., Trueman, C.N., 2015. Quantifying physiological influences on otolith microchemistry. Methods Ecol. Evol. 6, 806–816. https://doi.org/10.1111/2041-210X.12381.
- United States Geological Survey (USGS), 2013. Microanalytical Reference Materials and Accessories. U.S. Geological Survey Geochemical Reference Materials and Certificates.

- Utne-Palm, A.C., Salvanes, A.G., Currie, B., Kaartvedt, S., Nilsson, G.E., Braithwaite, V. A., Stecyk, J.A., Hundt, M., Van der Bank, M., Flynn, B., Sandvik, G.K., 2010. Trophic structure and community stability in an overfished ecosystem. Science 329 (5989), 333-336
- Utne-Palm, A.C., Locatello, L., Mayer, I., Gibbons, M.J., Rasotto, M.B., 2013. An insight into the reproductive biology of the bearded goby *Sufflogobius bibarbatus*. J. Fish. Biol. 82 (2), 725–731.
- Van der Bank, M.G., Utne-Palm, A.C., Pittman, K., Sweetman, A.K., Richoux, N.B., Brüchert, V., Gibbons, M.J., 2011. Dietary success of a 'new'key fish in an overfished ecosystem: evidence from fatty acid and stable isotope signatures. Mar. Ecol. Prog. Ser. 428, 219–233.
- van Hulten, M., Dutay, J.C., Middag, R., de Baar, H., Roy-Barman, M., Gehlen, M., Tagliabue, A., Sterl, A., 2016. Manganese in the world ocean: a first global model. Biogeosci. Discuss. 14, 1–38.
- Vaquer-Sunyer, R., Duarte, C.M., 2008. Thresholds of hypoxia for marine biodiversity. Proc. Natl. Acad. Sci. USA 105 (40), 15452–15457.
- Vogel, R.M., Fennessey, N.M., 1994. Flow-duration curves. I: new interpretation and confidence intervals. J. Water Resour. Plann. Manag. 120 (4), 485–504.
- Wakefield, W.W., 1990. Patterns in the Distribution of Demersal Fishes on the Upper Continental Slope off Central California with Studies on the Role of Ontogenetic Vertical Migration in Particle Flux. Ph.D. thesis, Scripps Institution of Oceanography, University of California, San Diego, Calif.
- Walther, B.D., Thorrold, S.R., 2006. Water, not food, contributes the majority of strontium and barium deposited in the otoliths of a marine fish. Mar. Ecol. Prog. Ser. 311, 125–130.
- Walther, B.D., Kingsford, M.J., O'Callaghan, M.D., McCulloch, M.T., 2010. Interactive effects of ontogeny, food ration and temperature on elemental incorporation in otoliths of a coral reef fish. Environ. Biol. Fish. 89 (3), 441–451.
- Wickham, H., 2016. ggplot2: Elegant Graphics for Data Analysis. Springer-Verlag, New York, 2016.
- Wyrtki, K., 1962. The oxygen minima in relation to ocean circulation. In: Deep Sea Research and Oceanographic Abstracts, vol. 9. Elsevier, pp. 11–23. No. 1-2.
- Zamorano, P., Hendrickx, M.E., Toledano-Granados, A., 2007. Distribution and ecology of deep-water mollusks from the continental slope, southeastern Gulf of California, Mexico. Mar. Biol. 150 (5), 883–892.
- Zamorano, P., Hendrickx, N.E., Méndez, N., Gómez, S., Serrano, D., Aguirre, H., Madrid, J., Morales-Serna, F.N., 2014. La exploración de las aguas profundas del Pacífico mexicano: proyecto Talud. In: La frontera final: el océano profundo. Secretaría de Medio Ambiente y Recursos Naturales. Instituto Nacional de Ecología y Cambio Climático. México.